RI 8901

Bureau of Mines Report of Investigations/1984

A Surface Resistivity Method for Measuring Hydrologic Characteristics of Jointed Formations

By Patricia J. Leonard-Mayer

SAFETY AND HEALTH TECHNOLOGY CENTER
1984 OCT 15 AM 10 45

MSHA LIBRARY
P. O. BOX 25367
DENVER, CO 80225

UNITED STATES DEPARTMENT OF THE INTERIOR

Report of Investigations 8901

A Surface Resistivity Method for Measuring Hydrologic Characteristics of Jointed Formations

By Patricia J. Leonard-Mayer

UNITED STATES DEPARTMENT OF THE INTERIOR
William P. Clark, Secretary

BUREAU OF MINES
Robert C. Horton, Director

Library of Congress Cataloging in Publication Data:

Leonard-Mayer, Patricia J

A surface resistivity method for measuring hydrologic characteristics of jointed formations.

(Report of investigations ; 8901)

Bibliography: p. 43-44.

Supt. of Docs. no.: I 28.23:8901.

1. Joints (Geology). 2. Rocks–Electric properties. I. Title. II. Series: Report of investigations (United States. Bureau of Mines) ; 8901.

TN23.U43 [QE605] 622s [551.8'4] 84-600028

CONTENTS

	Page
Abstract	1
Introduction	2
Acknowledgments	3
Electrical resistivity	3
General concepts and literature review	3
Summary of theory for an anisotropic earth	6
Geoelectric section	8
Extension of theory to jointed formations	9
Self-potential	11
Physical model study	12
Procedure	12
Presentation of data	12
Results	12
Field investigations	14
Spring Valley, Fillmore County, MN	14
Description of study area	14
Description of fieldwork	18
Results	19
Azimuthal survey, site 1	19
Azimuthal survey, site 2	20
Azimuthal survey, site 3	21
Conclusions	24
Shannopin Mine, Greene County, PA	24
Description of study area	24
Description of fieldwork	26
Results	26
Azimuthal surveys	26
Horizontal profile	27
Conclusions	29
Neda and Beechwood sites, Dodge County, WI	29
Site descriptions and summary of site characteristics	29
Preliminary fieldwork	31
Results	33
Conclusions	37
Mystery Ridge and Mystery Cave, Fillmore County, MN	38
Site descriptions	38
Description of fieldwork	39
Results and conclusions	41
Conclusions	43
References	43
Appendix.--Nomenclature	45

ILLUSTRATIONS

1.	Current and equipotential distribution in a vertical plane along a line of electrodes on the surface of a homogeneous, isotropic earth	4
2.	Electrode arrays used in surface resistivity surveys	6
3.	Coordinate system for a homogeneous, anisotropic earth with current applied at origin	7
4.	Relationship of true and apparent resistivities, and equation for the coefficient of anisotropy for a vertically layered formation	8

ILLUSTRATIONS--Continued

		Page
5.	Geoelectric section for a layered formation	9
6.	Geoelectric section for a single, uniform joint set	10
7.	Diagram of board matrix and electrode array used in laboratory model study of joint resistivity	13
8.	Apparent resistivity graph from azimuthal Wenner survey of board model	14
9.	Index map and site map, Spring Valley study area, Fillmore County, MN	14
10.	Site 1, Spring Valley study area	15
11.	Cedar Valley Limestone exposed in an abandoned quarry near Spring Valley study area	16
12.	Sinkhole exposed in active quarry near Spring Valley study area	17
13.	Rose diagram of joint measurements made in a southeast Minnesota joint study	18
14.	Portion of drainage map of South Branch, Root River, including Spring Valley, Mystery Ridge, and Mystery Cave study areas	18
15.	Perpendicular, vertical profiles, site 1, Spring Valley study area	19
16.	Wenner and Lee apparent resistivity graphs from azimuthal Wenner-Lee surveys, site 1, Spring Valley study area, Minnesota	20
17.	Wenner apparent resistivity graphs from azimuthal Wenner-Lee surveys, site 2, Spring Valley study area, Minnesota	21
18.	Horizontal profile, site 2, Spring Valley study area, Minnesota	21
19.	Wenner and Lee apparent resistivity graphs from azimuthal Wenner-Lee surveys, site 3, Spring Valley study area, Minnesota	22
20.	Self-potential, azimuthal survey, site 1, Spring Valley study area, Minnesota	23
21.	Self-potential, azimuthal survey, site 3, Spring Valley study area, Minnesota	23
22.	Site map and index map, Shannopin Mine, Greene County, PA	25
23.	Wenner and Lee apparent resistivity graphs from azimuthal Wenner-Lee surveys, Shannopin Mine, Greene County, PA	27
24.	Self-potential azimuthal surveys, stations 1 and 12a, Shannopin Mine, Greene County, PA	28
25.	Horizontal profile and stream gaging results, Shannopin Mine, Greene County, PA	28
26.	Index map and site map, Neda and Beechwood sites, Dodge County, WI	29
27.	Map of iron ore mine at Neda site, Dodge County, WI	30
28.	Rose diagram of joint survey at Beechwood site, Dodge County, WI	31
29.	Rose diagram of joint survey at Neda site, Dodge County, WI	32
30.	Rose diagram of lineaments measured on aerial photographs, Warzyn site, Dodge County, WI	32
31.	Precipitation at West Bend, WI, 1981-82	32
32.	Results of east-west depth sounding at Beechwood site	33
33.	Results from north-south depth sounding at Beechwood site using a Wenner array	33
34.	Results from north-south depth sounding at Neda site using a Wenner array	34
35.	Wenner apparent resistivity graphs from azimuthal Wenner surveys, Beechwood site, Wisconsin	34
36.	Wenner and Lee apparent resistivity graphs from azimuthal Wenner-Lee surveys, Beechwood site, Wisconsin	35
37.	Wenner apparent resistivity graphs from azimuthal Wenner surveys, Neda site, Wisconsin	36
38.	Wenner and Lee apparent resistivity graphs from azimuthal Wenner-Lee surveys, Neda site, Wisconsin	37

ILLUSTRATIONS--Continued

Page

39. Rose diagram of cave passage orientations, Mystery Ridge, Fillmore County, MN..... 39
40. Rose diagram of joint orientations, for joints intersecting cave passages, Mystery Ridge, Fillmore County, MN..... 39
41. Quarry near Spring Valley, MN, with Dubuque and Galena Formations exposed. 40
42. Wenner and Lee apparent resistivity graphs from azimuthal Wenner-Lee surveys, Mystery Ridge site, Minnesota..... 41
43. Wenner and Lee apparent resistivity graphs from azimuthal Wenner-Lee surveys, Mystery Cave site, Minnesota..... 42
44. Self-potential, azimuthal survey, Mystery Cave site, Minnesota..... 42

TABLES

1. Coefficients of anisotropy for rocks having a single, uniform joint set... 10
2. General geology from driller's logs and core description, near site 2, Spring Valley, Fillmore County, MN..... 15
3. Joint strike data, Spring Valley study area, Fillmore County, MN..... 16
4. Azimuths of relative maximum apparent resistivity, Spring Valley, site 1.. 20
5. Azimuths of relative maximum apparent resistivity, Spring Valley, site 2.. 21
6. Azimuths of relative maximum apparent resistivity, Spring Valley, site 3.. 22
7. General geology, Shannopin Mine, Greene County, PA..... 24
8. Average strike of joints and coal cleat, Shannopin Mine, Greene County, PA 25
9. Strike of joints and fractures at field site, Shannopin Mine, Greene County, PA..... 26
10. Azimuths of relative maximum apparent resistivity, Shannopin Mine..... 27
11. General geology, Neda and Beechwood sites, Dodge County, WI..... 30
12. Porosity and permeability, Neda and Beechwood sites, Dodge County, WI..... 33
13. Azimuths of 1981 relative maximum apparent resistivity, Beechwood site.... 34
14. Azimuths of 1982 relative maximum apparent resistivity, Beechwood site.... 35
15. Azimuths of 1981 relative maximum apparent resistivity, Neda site..... 36
16. Azimuths of 1982 relative maximum apparent resistivity, Neda site..... 37
17. General geology, Mystery Ridge and Mystery Cave sites, Fillmore County, MN 38
18. Azimuths of relative maximum apparent resistivity, Mystery Ridge site..... 41
19. Azimuths of relative maximum apparent resistivity, Mystery Cave site..... 42

UNIT OF MEASURE ABBREVIATIONS USED IN THIS REPORT

amp	ampere	km	kilometer
cm	centimeter	m	meter
cm/s	centimeter per second	m/s	meter per second
deg	degree	mV	millivolt
gpm	gallon per minute	ohm-m	ohm-meter
in	inch	pct	percent

A SURFACE RESISTIVITY METHOD FOR MEASURING HYDROLOGIC CHARACTERISTICS OF JOINTED FORMATIONS

By Patricia J. Leonard-Mayer [1]

ABSTRACT

A Bureau of Mines surface resistivity method has been used to determine the joint strike and coefficient of anisotropy of jointed, near-surface formations at five study areas. The field studies demonstrate the use of rotated, or azimuthal, Wenner-Lee arrays for determining the strike of predominant joint sets. The results of the field studies include the following: in a formation having a predominant, vertical joint set, the maximum value of the apparent resistivity (ρ_a) occurs in the same direction (azimuth) as the joint strike; the polar coordinate graph of ρ_a for such a formation is approximately elliptical; the coefficient of anisotropy (λ) can be calculated from the field data, and values of λ for jointed formations are in the same range of values reported for layered formations; values of λ are higher at mined sites than at unmined sites. The azimuthal resistivity method and horizontal profiling were used at a site in Pennsylvania to delineate a zone of intensely jointed and fractured bedrock that provided a flow path from a surface stream to a mine. Analysis of the data has been based on a simple model of a jointed formation having a single joint set; the success achieved to date indicates the need for a more complex model and additional field data.

[1]Hydrologist, Twin Cities Research Center, Bureau of Mines, Minneapolis, MN (now with the State of Minnesota, Department of Health, Minneapolis, MN).

INTRODUCTION

A thorough understanding of the natural ground water system is needed for planning an environmentally and economically sound mining operation. Hydrologic information is needed in developing the most efficient and practical mine plan, to predict and avoid any hazardous or undesirable water problems, to predict the volume of mine drainage to be handled during mining, as well as the resulting drawdown in the vicinity of the mine, and to predict any permanent changes in ground water and surface water flow systems. These factors contribute to the costs of the mining operation, as well as the additional costs of operating mine drainage treatment systems, pumping, recharge, and land and ground water reclamation and restoration.

In much of the Eastern bituminous coal fields the dominant ground water flow in coal and overburden is along fractures: in joints, faults and brecciated zones. In the Midwest, mines, quarries, and overburden are frequently jointed and sometimes faulted. In these cases, ground water flow is partly or wholly controlled by fractures. Locating fractures and accurately measuring the fracture characteristics in order to predict flow can be difficult and expensive. Recognizing this difficulty, the Bureau has supported research to improve upon the field methods currently available.

A preliminary Bureau investigation established a procedure for accurately locating major fracture zones and selectively dewatering the zones in coordination with mine development (1).[2] The fracture zones were on the order of tens of meters in width and could be accurately located on aerial photographs.

The investigation reported here deals with joints that are on the order of millimeters and less in width. To predict flow through jointed formations, the joint characteristics, including average joint width, joint spacing, orientation, and filling must be known for each joint set in the formation.

Joints in flat-lying, near-surface sedimentary rocks provide little surface expression of the joint characteristics. A series of springs along a geologic contact can give some indication of joint spacing, but other large-scale features do not exist. Although joint orientations can be measured at outcrops, joint width and spacing can be accurately measured only on unweathered samples, such as cores. Although direct observation and measurement are always most desirable, the lack of available sampling sites and the cost of sampling indicated a need for indirect methods of observation and measurement. The purpose of this study is to establish indirect methods of measuring the hydrologic characteristics of a common type of overburden, near-surface, flat-lying, jointed sedimentary rocks. The methods initially evaluated were standard surface geophysics methods.

Early in this study, surface resistivity and seismic methods were compared (2). Apparent resistivities and seismic velocities were measured at various orientations with respect to the known strike of a joint set.

It was found that apparent resistivity varied significantly with respect to orientation of joints at field sites and on laboratory models. The changes could be accounted for, qualitatively, by existing theory and were repeatable over time. The results from seismic methods were not as repeatable and could not be as easily explained. Surface resistivity was the principle method used throughout the remainder of the study.

[2]Underlined numbers in parentheses refer to items in the list of references preceding the appendix.

ACKNOWLEDGMENTS

Calvin Alexander, Department of Geology and Geophysics, University of Minnesota, Minneapolis, MN, and the Spring Valley Landowners Association, Fillmore County, MN, are thanked for their assistance in the portions of this study pertaining to southeastern Minnesota, particularly in gaining access to test sites. Owners of Mystery Cave, Fillmore County, MN, and Shannopin Mine, Greene County, PA, are thanked for granting permission to conduct tests on their property.

ELECTRICAL RESISTIVITY

GENERAL CONCEPTS AND LITERATURE REVIEW

For most rocks near the earth's surface, electrical conduction due to a current impressed at the surface is electrolytic, where the solution of common salts distributed through the rock in interconnected pores or joints serves as an electrical conductor. The solid rock matrix offers resistance to electrical flow. The surface electrical resistivity method is a prospecting method in which current is impressed into the ground and the effects of the current are obtained by measuring potential differences at the ground surface.

Many of the surface resistivity methods used, including all of the work done in this study, employ two current electrodes and two potential electrodes. The electrodes are arranged in any one of a number of configurations called arrays. The fundamental theory involved in surface resistivity methods is dependent upon the validity of Laplace's equation for describing the electrical potential and the pattern of current flow about the electrodes. The assumption of Laplace's equation implies that Ohm's law is applicable as well; that is, the resistance of the earth acting as a conductor is the same no matter what applied voltage is being used to measure it.

When two current electrodes are used, one acts as a current source, the other as a current sink. In a homogeneous isotropic earth, the resulting potentials are as shown in figure 1. Current flow lines are perpendicular to the lines of equal potential. In a layered or jointed earth, the flow and potential lines are deflected from this pattern at each interface depending upon the resistivities of the layers or of the unfractured blocks and joints. Current flow paths in a horizontal layered earth depend upon the layer thicknesses and layer resistivities; current flow paths in a jointed earth depend upon the joint width, spacings, and resistivities of the fluid or other joint filling, as well as the resistivity of the unfractured blocks.

For any arrangement of electrodes on the earth's surface, a mathematical expression relating the potential, the impressed current, and the geometry of the electrode array to another variable, called the apparent resistivity, can be derived. In practice, apparent resistivity values are calculated from field measurements that were obtained as the geometry of the array was changed in some way.

The usual objective in conducting a resistivity survey in layered rocks is to interpret the apparent resistivities and electrode spacings to provide the depth to interfaces between electrically distinct units. A second objective is to characterize the units (identify rock type, porosity, or another property). In another type of resistivity work, apparent resistivities and array geometries are interpreted to provide the depth and size of a body imbedded in a homogeneous, isotropic earth.

Theory and methods of interpretation are thoroughly explained in standard references (3-5). In the past, interpretation of apparent resistivity data was carried out according to a variety of empirical methods or by curve matching. Today, curve matching is the principal

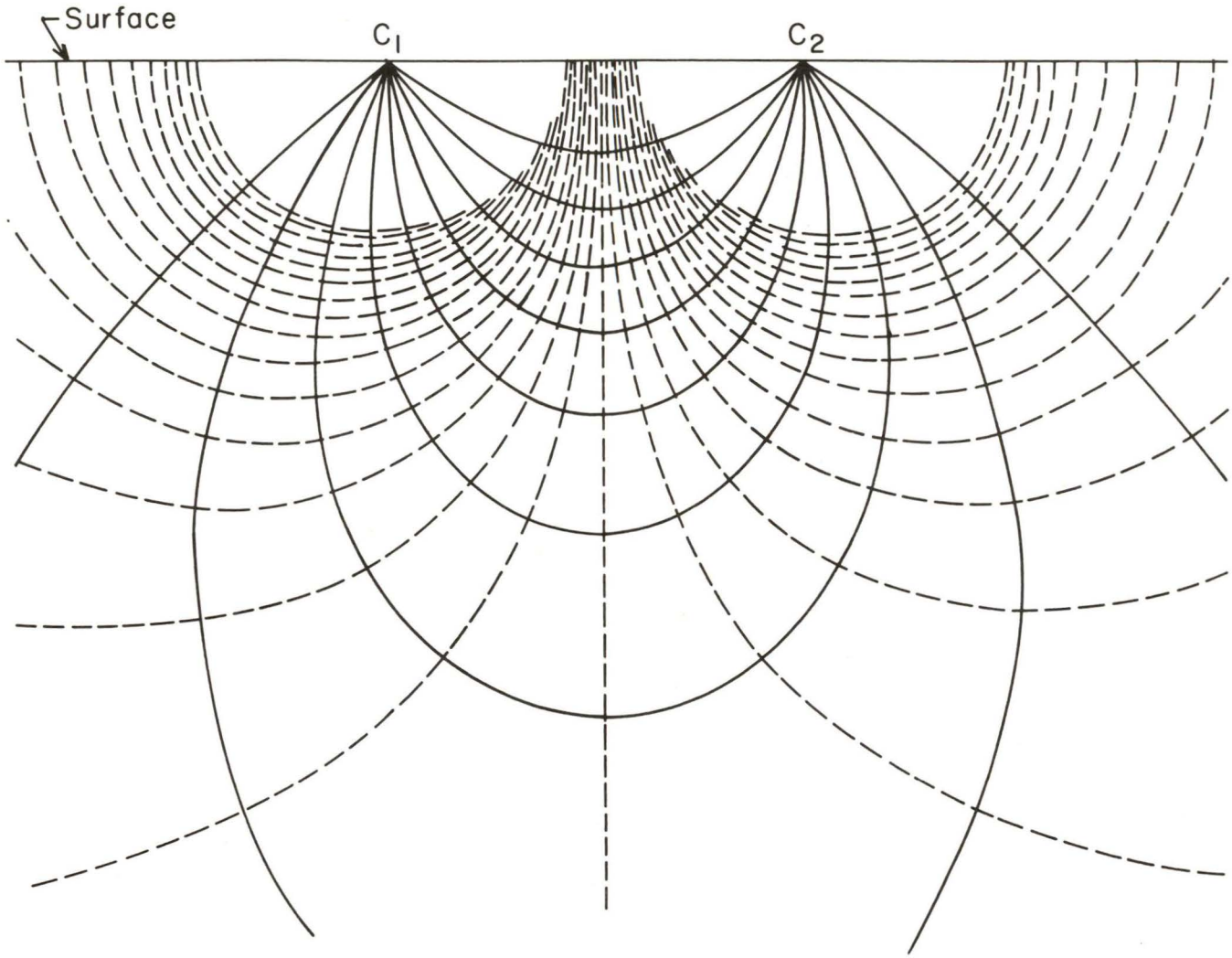


FIGURE 1. - Current (solid lines) and equipotential (dashed lines) distribution in a vertical plane along a line of electrodes on the surface of a homogeneous, isotropic earth.

method of interpretation, usually carried out by means of computer-generated curves.

In order to apply the surface resistivity method to common hydrologic problems, the layered-earth concept can often be used. Layers of interest, such as zones of contaminated ground water, are treated as separate layers having a given thickness and true resistivity. Determining depth to a saltwater interface, for example, is similar to determining depth to a lithologic interface. Use of this approach along with available computer programs in the planning stages of a project and in interpretation of field data can be extremely useful. Attempts to use the resistivity method in hydrologic applications without a conceptual model and without a sound method of calculation are frequently unsuccessful. This may account for some dissatisfaction with the resistivity method on the part of hydrologists.

Little attention has been paid in resistivity studies to the problem of anisotropy, although it has been recognized for decades that isotropy is not often encountered in practice. The importance of understanding the effects of anisotropy were pointed out early in the development of resistivity theory (6):

> ...it is very desirable for the geophysicist to have quite an extensive knowledge of the properties of anisotropic formations, and of the laws that govern the propagation of electrical current therein. With such principles in mind, he will be able to decide whether the conclusions arrived at in simple, isotropic conditions are still correct in more complex cases, or in what way they must be modified or adapted in order to constitute a sound basis for the interpretation of the results obtained in anisotropic media.

The utility of anisotropic effects was also realized at that time (6),

> ...the fact that in anisotropic formations the mobility of the ions is greater along the strike than perpendicular thereto can be utilized for determining the direction of the dip by induction measurements.

Applied potential techniques have since been developed in order to determine dip (7). The effects of anisotropy in electrical resistivity surveys of layered rocks have been studied, and resistivity arrays have been developed in order to determine strike of dipping beds under alluvial cover (8). The effects of anisotropy have generally been overlooked in electrical resistivity surveys of jointed rocks, however.

The literature regarding electrical resistivity anisotropy of jointed rocks is very limited. Reference 3 includes a brief, general discussion in its introduction but does not treat the subject in detail in the section on anisotropy. The other general texts available in English do not discuss anisotropy due to jointing. At least one Soviet text (9) discusses the topic briefly, including description of a field procedure similar to the method developed in this study (see especially pp. 205-215). Two papers (10-11) examine the relationship between electrical resistivity anisotropy and fractured rock characteristics. The rocks of interest in these papers are deep petroleum reservoirs; therefore, the description of the fractured rock system and the information sought by use of the method are different from those in this project. Additional information is undoubtedly available in the Soviet literature, but it has not been possible to locate additional references.

A rotated array, similar to the one developed in this study (and attributed to Soviet sources), was used in a study of limestones (12). Although the authors intended to measure the resistivity effects of large solution cavities, it is likely that they have measured effects of the jointed rock in which solution features have developed. Rotated Wenner and Schlumberger arrays were used in a study (13) to determine an azimuth-apparent resistivity relationship. The formations studied consisted of steeply dipping, jointed metagraywacke and metagraywacke interbedded with quartzite. The effect on apparent resistivity due to jointing alone could not be separated from the effects of lithology, structure, and topography.

The purpose of this study is to establish surface resistivity methods for measuring the hydrologic characteristics of jointed formations. To accomplish this, electrical resistivity anisotropy must be considered. Although the literature indicates that sedimentary layers measurably affect apparent resistivity (in a manner that is explained more thoroughly in the next section) only a limited amount of information is available concerning the affects of joints on apparent resistivity. The literature indicates that it is very likely, however, that joints affect apparent resistivity in much the same way as layers do. The literature does not indicate a way to quantify and interpret the apparent resistivity data from jointed formations in a way that would yield the information needed

to predict flow. The equations and parameters used to describe an anisotropic layered earth are summarized in the next section. These concepts are then extended to the jointed formation to show how resistivity and joint characteristics, such as joint width, can be related to one another. A more detailed statement of the purpose of the study is given prior to the sections describing field studies.

SUMMARY OF THEORY FOR AN ANISOTROPIC EARTH

Detailed derivations of the following equations are available in geophysics textbooks and will not be repeated here; for completeness, however, a brief discussion is presented. For a homogeneous and isotropic earth, the potential measured at the earth's surface due to a single current electrode is given by

$$U = \frac{\rho I}{2\pi r}, \qquad (1)$$

where U is the potential (volts) measured at some point of interest, ρ is the resistivity (ohm-meters), I is current (amperes), and r is the distance (meters) from the current source to the point of interest. Potential functions are scalars and therefore may be added arithmetically. The total potential at a point on the earth's surface due to n current sources is given by

$$U = \frac{\rho}{2\pi}\left\{\frac{I_1}{r_1} + \frac{I_2}{r_2} + \cdots + \frac{I_n}{r_n}\right\}, \qquad (2)$$

where I_n is the current from the nth current electrode and r_n is the distance from the nth source at which the potential is being observed. This equation can be used to determine the potential differences between any two potential electrodes. For the arrays most often used, the following equations apply:

$$V_W = \frac{\rho I}{2\pi a}, \qquad (3)$$

$$V_L = \frac{\rho I}{4\pi a}, \qquad (4)$$

and

$$V_S = \frac{\rho I a}{\pi L^2}, \qquad (5)$$

where V_W, V_L and V_S are the potential differences for the Wenner, Lee, and Schlumberger arrays, a is the electrode spacing, and where the electrode configurations are as illustrated in figure 2. Considering the Wenner array, resistivity is given by $\rho = 2\pi a\ V/I$ if the earth is completely homogeneous and isotropic. When the earth is not homogeneous and isotropic, this equation can be used to define apparent resistivity, $\rho_a = 2\pi a\ V/I$.

For a homogeneous, anisotropic earth, where the resistivity in the horizontal

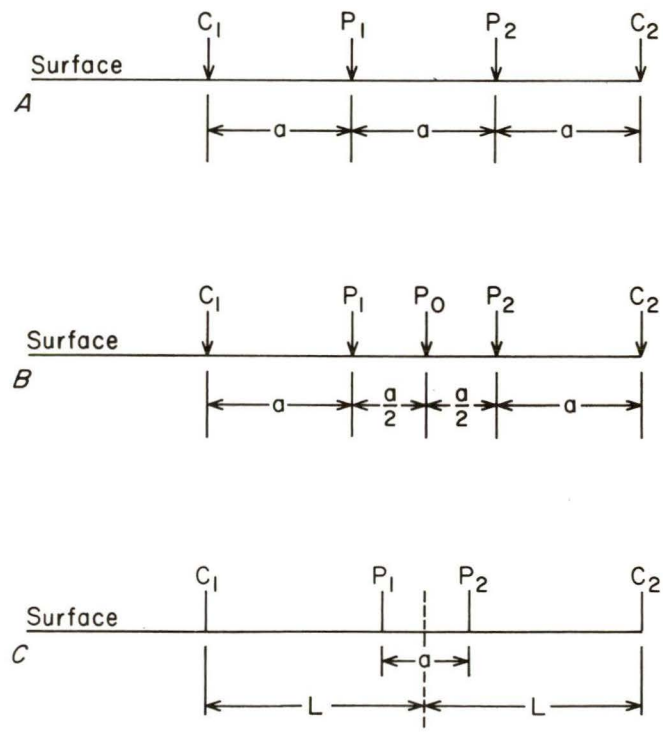


FIGURE 2. - Electrode arrays used in surface resistivity surveys. *A*, Wenner array, a is the electrode spacing; *B*, Lee array, similar to the Wenner array but includes a third potential electrode (the Lee and Wenner arrays are easily combined for use in the field); *C*, Schlumberger array, a is the potential electrode separation, L is the current electrode separation, and L>>a.

directions, x and y, is ρ_ℓ (called the longitudinal resistivity) and the resistivity in the vertical direction, z, is ρ_t (the transverse resistivity), the potential measured at the earth's surface due to a single current electrode is given by

$$U = \frac{I\lambda\rho_\ell^{3/2}}{2\pi\rho_\ell^{1/2}\,(x^2 + y^2 + \lambda^2 z^2)^{1/2}}, \quad (6)$$

where λ is the coefficient of anisotropy, $\lambda = (\rho_t/\rho_\ell)^{1/2}$, and where the current is applied at the origin of the cartesian coordinate system (fig. 3). The equation for an equipotential surface is given by

$$x^2 + y^2 + \lambda^2 z^2 = \left[\frac{I\lambda\rho_\ell}{2\pi U}\right]^2 = \text{constant}, \quad (7)$$

which describes an ellipse rotated around the z-axis. The potential at a point on the earth's surface is given by

$$U = \frac{I\lambda\rho_\ell}{2\pi r}, \quad (8)$$

where r is the distance from the current source to the point of interest. The apparent resistivity at this point is

$$\rho_{a_\ell} = 2\pi r\,\frac{U}{I} = \lambda\rho_\ell. \quad (9)$$

The potential at a point of interest on the z-axis (supposing a vertical cliff exists) is given by

$$U = \frac{I\rho_\ell}{2\pi r}, \quad (10)$$

and the apparent resistivity is

$$\rho_{a_t} = 2\pi r\,\frac{U}{I} = \rho_\ell. \quad (11)$$

First, from equation 9, it can be seen that the resistivity measured on the earth's surface over horizontal beds, ρ_{a_ℓ}, will be larger than the true longitudinal resistivity, ρ_ℓ, by a factor equal to λ. From equation 11, the resistivity measured on the earth's surface over vertical beds, in a direction perpendicular to bedding, is equal to the true longitudinal resistivity, ρ_ℓ. This result is known as the paradox of anisotropy. The phenomenon is explained in reference 6. Another important result is that while the ratio $\rho_t/\rho_\ell = \lambda^2$, the ratio $\rho_{a_\ell}/\rho_{a_t} = \lambda$. The relationship of the true resistivity ellipse and the apparent resistivity ellipse is illustrated in figure 4.

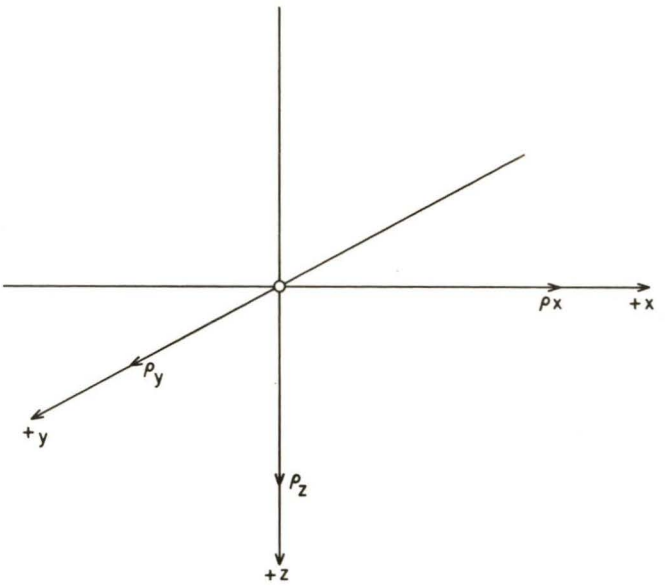


FIGURE 3. - Coordinate system for a homogeneous, anisotropic earth with current applied at origin.

The effect of these parodoxical results on field interpretation have been pointed out (3). First, if resistivity methods are being used to determine the strike of vertical or steeply dipping beds under sediment, the maximum apparent resistivity measured will be in the direction of the strike of the beds, and the minimum apparent resistivity will be measured in a direction at right angles to strike. Second, in resistivity soundings over shallow dipping or horizontal layers, the interpreted resistivity resulting from apparent resistivity measurements will be larger than the true longitudinal resistivity, and the interpreted thickness will be greater than the true thickness, by a factor equal to λ, the coefficient of anisotropy.

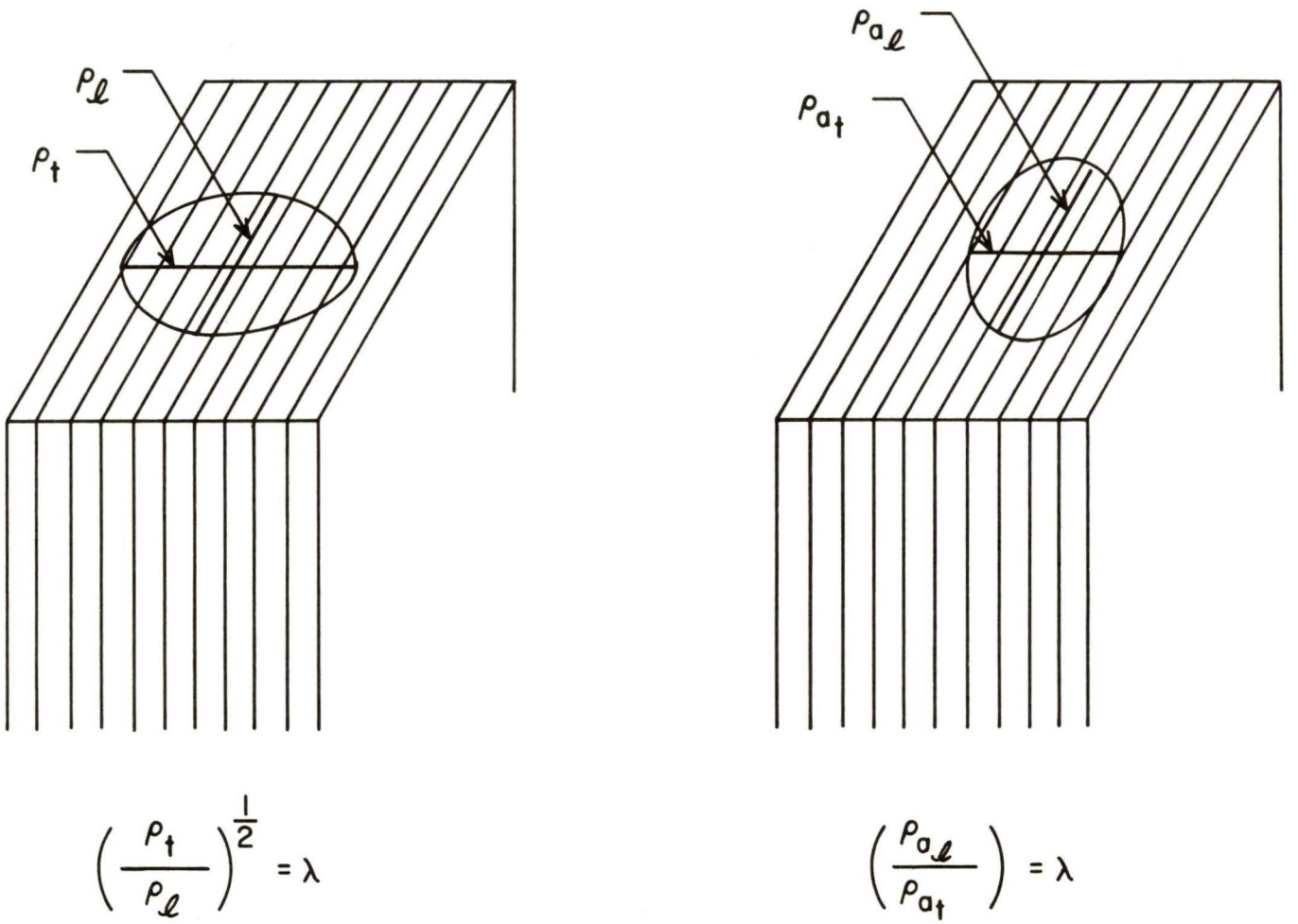


FIGURE 4. - Relationship of true and apparent resistivities, and equation for the coefficient of anisotropy for a vertically layered formation.

GEOELECTRIC SECTION

Inhomogeneity and anisotropy of layered rocks are sometimes taken into account by means of the parameters of the geoelectric section. A column of layered rock 1 m on a side and extending through the entire thickness, H, of the section, is described in terms of its layer resistivities, ρ_i, and thicknesses, h_i (fig. 5). The resistance (R) to current flow through a single layer in the vertical direction is given in general by

$$R_i = \rho_i \frac{L}{A}, \qquad (12)$$

where L is the distance that the current flows through the layer and A is the cross sectional area. Therefore, in this case

$$R_i = \rho_i h_i. \qquad (13)$$

The transverse resistance, T, is the sum of resistances of all beds in the section:

$$T = \Sigma\, \rho_i h_i. \qquad (14)$$

The average resistivity in the direction perpendicular to bedding is the transverse resistivity, ρ_t,

$$\rho_t = \frac{T}{H} = \frac{\Sigma\, \rho_i h_i}{\Sigma\, h_i}. \qquad (15)$$

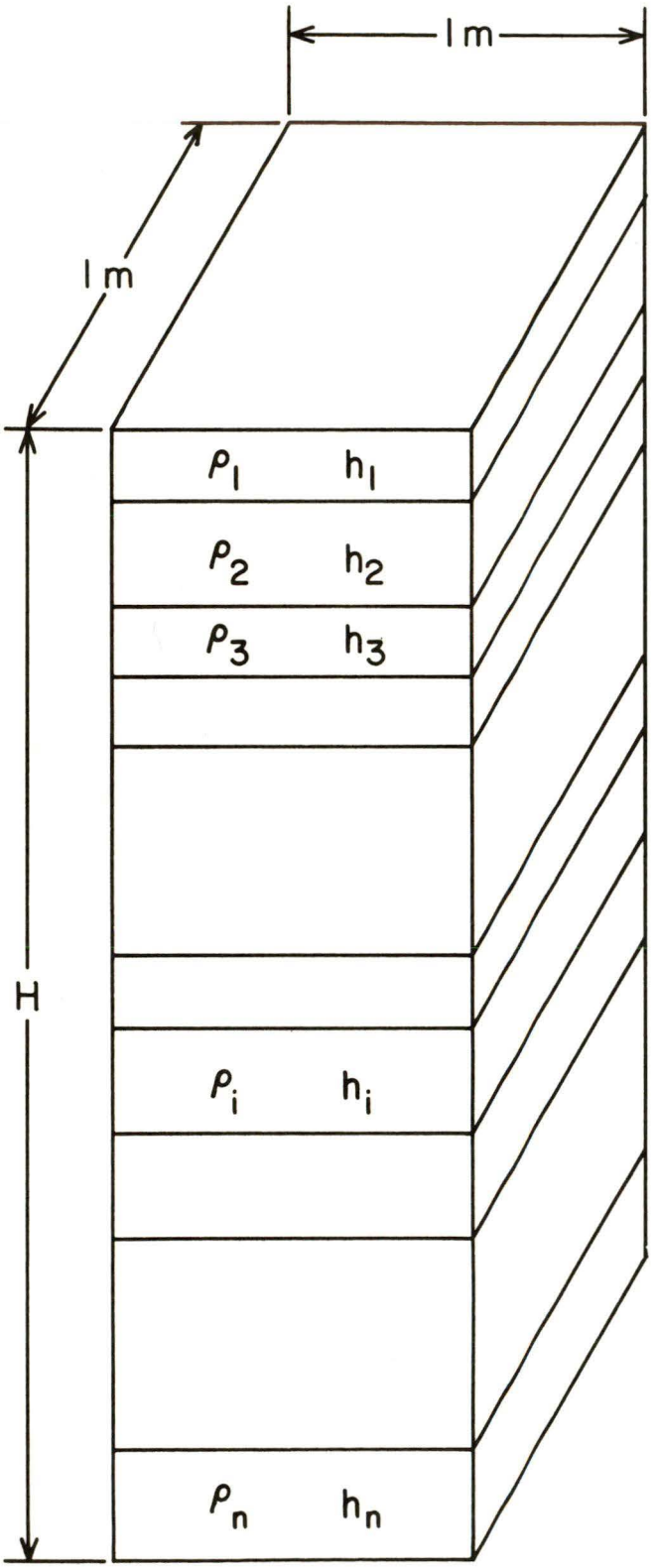


FIGURE 5. - Geoelectric section for a layered formation.

The conductance for current flowing parallel to bedding through an individual layer is given by

$$\frac{1}{R_i} = \frac{1}{\rho_i} \frac{A}{L} \tag{16}$$

or

$$\frac{1}{R_i} = \frac{h_i}{\rho_i}. \tag{17}$$

The total conductance in the direction parallel to bedding, S, is given by

$$S = \Sigma \left[\frac{h_i}{\rho_i} \right]. \tag{18}$$

The average conductivity corresponding to equation 18 is given by

$$\sigma_\ell = \frac{S}{H}. \tag{19}$$

The average resistivity in the direction parallel to bedding is

$$\rho_\ell = \frac{H}{S} = \frac{\Sigma\, h_i}{\Sigma \left[\frac{h_i}{\rho_i} \right]}. \tag{20}$$

The longitudinal resistivity, ρ_ℓ, is always smaller than the transverse resistivity, ρ_+. The coefficient of anisotropy, λ, given by

$$\lambda = (\rho_+/\rho_\ell)^{1/2}, \tag{21}$$

is greater than or equal to 1. (λ is equal to 1 in the case of an isotropic earth.) The five parameters used to describe a geoelectric section are T, ρ_+, S, ρ_ℓ, and λ.

EXTENSION OF THEORY TO JOINTED FORMATIONS

The theory of electrical resistivity anisotropy and the geoelectric parameters, described in the preceding sections, apply to layered formations. If a ground-water-saturated joint is thought of as a layer having very small thickness and low resistivity, then a formation having a single joint set is a "layered

formation" and the equations and methods of interpretation from the previous sections can be applied to it. The geoelectric parameters for a single set of regularly spaced joints having constant joint width (fig. 6) can be calculated according to equations 14 through 21, which can be simplified to the following:

$$\rho_t = \frac{\{\rho_1 h_1 + \rho_2 h_2\}\, N}{(h_1 + h_2)\, N} = \frac{\rho_1 h_1 + \rho_2 h_2}{h_1 + h_2}, \quad (22)$$

$$\rho_\ell = \frac{(h_1 + h_2)\, N}{\left[\frac{h_1}{\rho_1} + \frac{h_2}{\rho_2}\right] N} = \frac{h_1 + h_2}{\frac{h_1}{\rho_1} + \frac{h_2}{\rho_2}}, \quad (23)$$

$$\text{and} \quad \lambda^2 = \frac{(\rho_1 h_1 + \rho_2 h_2)\left[\frac{h_1}{\rho_1} + \frac{h_2}{\rho_2}\right]}{(h_1 + h_2)^2}, \quad (24)$$

where the section has N joint-block pairs. Equations 22 through 24 have been used to calculate resistivities and the coefficients of anisotropy for reasonable values of ground water and bulk rock resistivity, joint width, and joint spacing (block width) (table 1). The coefficients of anisotropy are between 1.01 and 1.49, well within the range of values for layered rocks (3). This provides one justification for proceeding with the analogy.

If the analogy between joints and layers is valid, the paradox of anisotropy can be applied in practical problems to determine the strike of vertical joints under alluvial cover, and a value of anisotropy can be calculated from apparent resistivities (according to $\rho_{a_\ell}/\rho_{a_t} = \lambda$). This information is useful in hydrologic analyses because the joint strike indicates the principal flow direction and the coefficient of anisotropy provides a convenient means for comparison of different formations. According

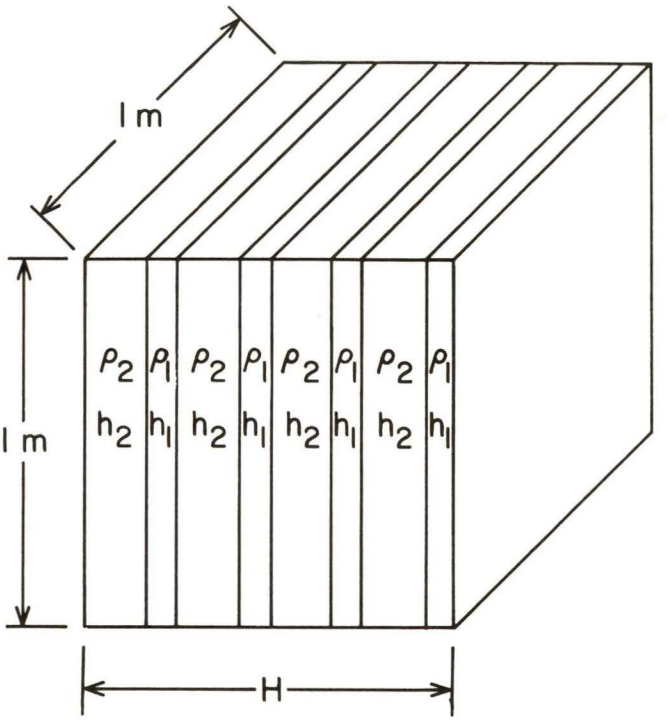


FIGURE 6. - Geoelectric section for a single, uniform joint set. Joint width and true resistivity are indicated as h_1 and ρ_1. The width and true resistivity of the blocks are h_2 and ρ_2.

TABLE 1. - Coefficients of anisotropy for rocks having a single, uniform joint set

(Equations 22 through 23 are used for the calculations)

ρ_1,[1] ohm-m	h_1, m	ρ_2,[2] ohm-m	h_2, m	ρ_t, ohm-m	ρ_ℓ, ohm-m	λ
100	0.0005	50,000	0.9995	49,975	40,016	1.12
50	.001	5,000	.449	4,989	4,098	1.10
100	.0005	250,000	.0995	24,876	11,136	1.49
50	.0005	5,000	1.995	4,999	4,879	1.01
100	.001	10,000	.1	9,902	5,050	1.40

[1]Estimated ground water resistivity.
[2]Unfractured rock (chemical precipitates) (3, p. 40).

to equation 24, different values of λ could result from a change in joint width or joint spacing (block width) when the ground water and bulk rock resistivities are constant.

The joint width is the jointed rock characteristic that is the most difficult to measure in the field, yet it is critical for calculating flow because flow varies with joint width raised to the third power (14). Treating joints as very thin layers provides a means of relating a joint width to true resistivities and, therefore, to apparent resistivities. Equation 24 can be rearranged as follows:

$$h_1 = \frac{-\left(\frac{\rho_1 h_2}{\rho_2} + \frac{\rho_2 h_2}{\rho_1} - 2\lambda^2 h_2\right) \pm \left[\left(\frac{\rho_1 h_1}{\rho_2} + \frac{\rho_2 h_2}{\rho_1} - 2\lambda^2 h_2\right)^2 - 4h_2^2(1-\lambda^2)^2\right]^{1/2}}{2\,(1-\lambda^2)} \quad . \quad (25)$$

The overall purpose of this study is to establish surface resistivity methods for measuring the hydrologic characteristics of a jointed formation. The first step toward that goal is to determine whether it is correct and useful to treat joints as thin layers in electrical resistivity studies. At each field site, the measured orientation of the predominant joint set would be compared to the direction of the maximum apparent resistivity. Coefficients of anisotropy would also be calculated from apparent resistivities. If the theory of anisotropy applies (the maximum apparent resistivity being in the direction of the joint strike) and reasonable coefficients of anisotropy result, this "thin layer" approach to joint evaluation will be justified. One potential problem with the approach is the fact that most jointed formations have more than one joint set. The effect of two, three, or more joint sets on the apparent resistivity is not known. Many jointed rocks have a single predominant joint set, however, and the effect of that joint set on the apparent resistivity is expected to be predominant as well.

SELF-POTENTIAL

Streaming potential is the potential developed in a liquid when it is forced through a capillary or filter. The phenomenon is explained in detail in reference 15. Streaming potentials associated with ground water flow through porous and fractured media have been reported. Negative electric potentials resulting from downward water movement have been successfully used in coordination with other methods to detect leaks in reservoirs (16). Significant negative potentials are expected in karst regions, where water is lost in sinkholes, and near the cones of depression from pumping wells; positive potentials are associated with ground water discharge zones (17). A limited amount of laboratory work has been done to relate fracture width and filling to measured streaming potentials (18).

Throughout the study, naturally occurring self-potentials (SP's) were measured in most of the azimuthal surveys. The purpose of the measurements was to determine whether anomalous natural potentials occurred at the sites, and, if so, to determine what relationship the potentials had to the apparent resistivities and the joint orientations. The correct method for measuring natural potentials is by means of "porous pot" electrodes. Porous pot electrodes eliminate the electrochemical potential due to interaction between a metal electrode and the earth. Because time in the field was limited, and because this work was of secondary importance in the project, porous pots were not used. All of the SP data have some unknown error owing to the use of metal electrodes. Naturally occurring potentials can also occur because of chemical reactions between an ore body and the surrounding rock; this reaction was not expected at the sites selected for this study.

PHYSICAL MODEL STUDY

A physical model study was conducted prior to initiating field investigations. The purpose of the model study was to determine whether the paradox of anisotropy applies to a medium containing a single, vertical joint set. The model was built from wooden boards spaced to form joints 1/4-in-wide with joint strike in an east-west direction (fig. 7). The joints were filled with a fine- to medium-grained sand; an inch of sand was placed on top of the board matrix. The model was built in a tank that could be filled to the desired water level. Three water levels were used in the study. The physical model and test results have been described in detail in reference 2.

PROCEDURE

A Wenner resistivity array with an electrode spacing of 10.2 cm was set up along a north-south line on the surface of the model, and the current and potential were measured and recorded. The array was then rotated about its midpoint to a position N10°E and the current and potential at that array orientation were measured. The procedure was repeated until a rotation of 180° was completed and the array was again on a north-south line. The electrode spacing was kept constant for the entire set of measurements. Until recently, inadequate resolution by resistivity instruments blocked attempts to measure differences in resistivity with direction. Signal-enhancement features have been added to resistivity instruments to eliminate effects of natural earth currents, extraneous potentials at contacts between electrodes and the earth, electromagnetic coupling, and induced polarization. Measurements were made with one such unit, a Bison[3] resistivity system (2390) that had been slightly modified to reduce the current output.

PRESENTATION OF DATA

For each set of data (that is, for each 180° rotation made with a constant electrode spacing) apparent resistivities were calculated and plotted in polar coordinates. In order to delineate the directions of significantly higher apparent resistivity on the graphs, the average value of apparent resistivity was calculated for the data set and values of apparent resistivity greater than 5 pct above the average are indicated by a line across the graph. These resistivity peaks or "maxima" must be accounted for in the interpretation of the model or field site investigation.

RESULTS

The apparent resistivity of the physical model was found to be slightly greater in the direction of the joint strike (fig. 8). In only one case, however, was the increase greater than 5 pct above the average apparent resistivity. Coefficients of anisotropy resulting from the three tests were 1.07, 1.04, and 1.11. The physical model study showed that the maximum apparent resistivity was in the direction of the joint strike, as predicted by the theory of resistivity anisotropy. An overall decrease in apparent resistivity was expected as the water depth increased and the model became more completely saturated and conductive. The increase in resistivity for the water depth of 16.5 cm was therefore unexpected and cannot be explained at this time. The joint-width-to-board-width ratio in the physical model was probably too high and the joint-resistivity-to-board-resistivity ratio too low to be considered a realistic model of jointed rock.

[3]Reference to specific trade names or manufacturers does not imply endorsement by the Bureau of Mines.

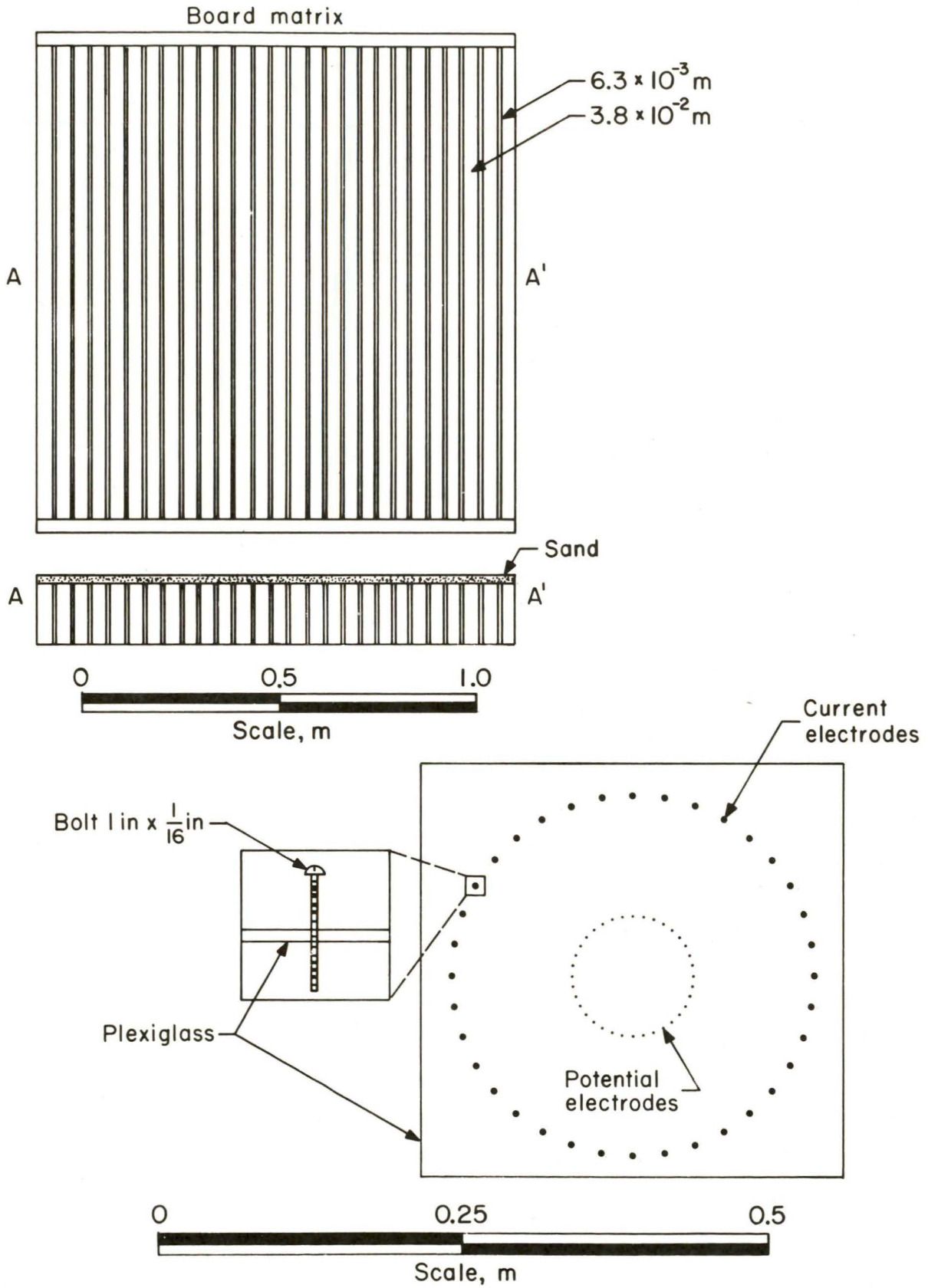


FIGURE 7. - Diagram of board matrix and electrode array used in laboratory model study of joint resistivity (2).

FIELD INVESTIGATIONS

SPRING VALLEY, FILLMORE COUNTY, MN

Description of Study Area

Field investigations were conducted near Spring Valley, MN, during the winter and spring of 1982. The area was selected for the investigation because the bedrock at the site has a structure similar to that assumed in the theoretical analysis (fig. 6): bedrock in the study area consists of flat-lying, vertically jointed carbonates; the water table is near the ground surface, providing fully saturated joints; a predominant joint set appears to be present in the multijointed formations. In addition, the topography of the area is relatively flat, which eliminates the need for a topographic correction to the resistivity data and reduces the overall effort needed to complete the fieldwork.

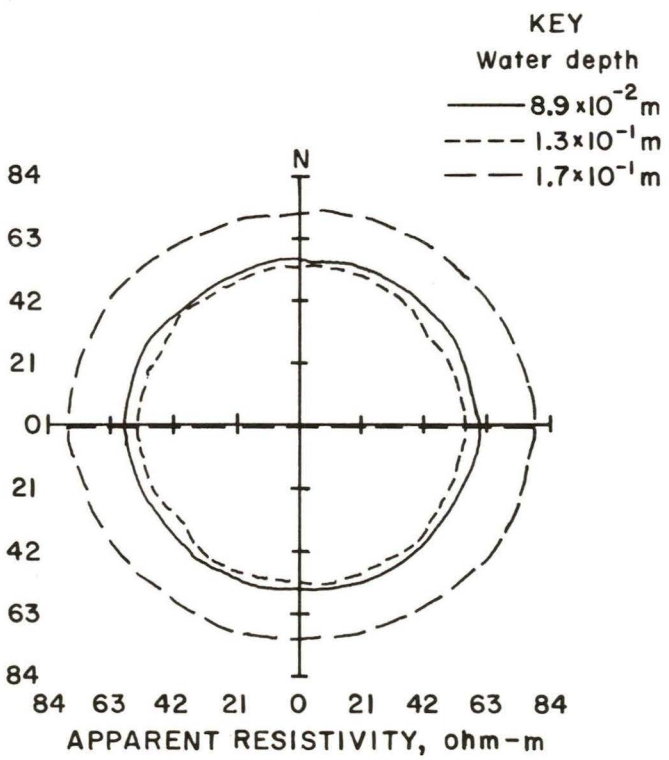


FIGURE 8. - Apparent resistivity graph from azimuthal Wenner survey of board model. All three graphs are elongated in the east-west direction, although only one has an increase greater than 5 pct above the average apparent resistivity for the entire survey (2).

Three resistivity survey sites were selected. The sites were on farmland adjacent to a sanitary landfill, which was constructed on a reclaimed open pit iron ore mine (figs. 9-10). Bedrock and soils at the resistivity survey sites were not disturbed by the mining operations, however. Fieldwork at the sites was conducted far from metal fences; other sources of interference, such as pipelines and powerlines were not located in the vicinity.

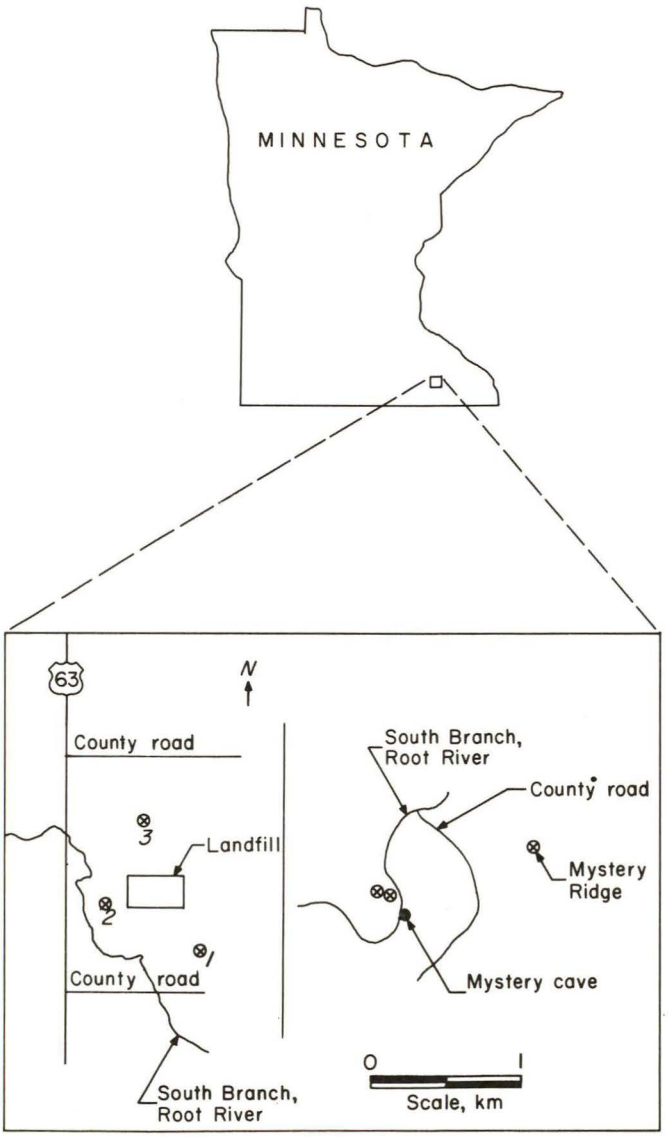


FIGURE 9. - Index map and site map, Spring Valley study area, Fillmore County, MN.



FIGURE 10. - Site 1, Spring Valley study area, looking north toward landfill dike land. *(Courtesy Ms. Pamela Watson)*

The formations of interest in the study are the Cedar Valley, Maquoketa, and Dubuque Formations. The lithologic descriptions and local thicknesses of the formations were available from State highway department records (table 2). The Cedar Valley Formation (Devonian) is a highly weathered limestone with an almost spongy appearance; vertical joints and solution features in the formation are apparent in a quarry located approximately 1 mile southeast of the survey sites (fig. 11). The Maquoketa and Dubuque Formations (Ordovician) are jointed limestones with interbedded shaley layers; the formations are exposed in a quarry located approximately 6 miles east of the survey sites (fig. 12). These formations and the underlying Galena Formation are characterized as karst in southeast Minnesota.

Joint strike information for the Cedar Valley, Maquoketa, and Dubuque Formations was obtained from the following sources: a survey of joint and cave orientations in Mystery Cave (20) (see also figures 39-40); a study of joint orientations in parts of three counties in southeast Minnesota (21) (see figure 13); and a stratigraphic study of the Cedar Valley Formation (22). Joints were also observed at local quarries, springs, and outcrops. There was no information available regarding the joint spacing, width, or filling (other than ground water).

A drainage map of the South Branch of the Root River, the watershed containing the study area, was prepared from topographic maps (fig. 14). The drainage map indicates that there is structural (joint) control of surface water in the basin. This is indicated by the presence of straight stream segments, sharp bends in the channel, and by the characteristic angles formed at stream junctions. There is a pronounced elongation of the stream network in an east-west direction.

TABLE 2. - General geology from driller's logs and core description, near site 2, Spring Valley, Fillmore County, MN (19)

Depth, m	Formation and/or description
0 to 2.13.....	Soil; frost to 0.8 m; slightly plastic to plastic sand loam.
2.13 to 5.79....	Cedar Valley Formation (Devonian); highly weathered limestone.
5.79 to 7.31....	Solon Member, Cedar Valley Formation (Devonian); weathered calcitic dolomite. Several natural horizontal and weathered vertical fractures, 6.10 to 7.13 m.
7.31 to 8.87....	Solon Member, Cedar Valley Formation (Devonian); calcitic dolomite.
8.87 to 12.83...	Maquoketa Formation (Ordovician); shaley dolomitic limestone. Shale layers at 9.66 to 9.81, 11.22 to 11.31, and 11.46 to 12.22 m. Bottom of hole at 12.83 m.



FIGURE 11. - Cedar Valley Limestone exposed in an abandoned quarry near Spring Valley study area. *(Courtesy Ms. Pamela Watson)*

Joint strike data are summarized in table 3. There is good agreement among the data from various sources. The N100°E joint set appears to be predominant in the study area, with secondary joint sets occurring in the N40°-50°E and N150°-160°E directions. A less clearly defined set probably occurs in the N120°E direction.

The water table in the area is near the surface, probably at depths of 10 m or less throughout the year. Depth to water in a domestic well near site 1 was about 5 m in the spring. Ground water elevation in bedrock monitoring wells at the sanitary landfill indicate that the water table slopes to the west (20). Some nearby farm fields drain internally to

TABLE 3. - Joint strike data, Spring Valley study area, Fillmore County, MN

Joint strike	Location of data collection sites
N100°E, N50°E, N150°-160°E (estimated from rose diagrams, figures 63-64).	Mystery Cave near Mystery Ridge, Fillmore County, MN (20).
N52.6°E, standard deviation 11°, N100.1°E, standard deviation 8.5°, diffuse peak at N120°E (total of 3,179 measurements, also see figure 14).	Southeastern Minnesota (21).
N40°E, E-W.....	Ordovician rocks in southeastern Minnesota and northern Iowa (22).
E-W, NE-SW, NW-SE.....	Drainage map interpretation, South Branch of Root River.



FIGURE 12. - Sinkhole exposed in active quarry near Spring Valley study area. The upper, thinner bedded formation is Maquoketa Formation; the lower, thicker bedded formation is Dubuque Limestone.
(Courtesy Ms. Pamela Watson)

sinkholes or to blind valleys; there was no surface expression indicating that sinkholes were present at any of the survey sites.

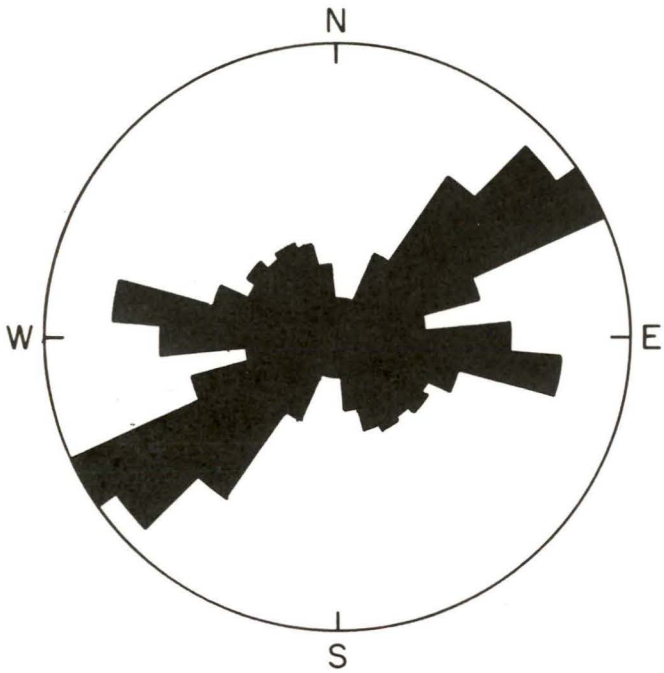


FIGURE 13. - Rose diagram of joint measurements made in a southeast Minnesota joint study (21).

Two trips were made to the study area, one in winter and one in the spring of 1982. A frost layer was present in the winter when the fieldwork was conducted.

Description of Fieldwork

Perpendicular vertical soundings were conducted at site 1 in March 1982. The soundings were used to quickly verify that directional differences in apparent resistivity occurred and were measurable, and to determine the electrode spacings where directional differences were at a maximum. Keeping the midpoint of the array fixed, a vertical survey was run on a north-south line, then another on an east-west line (fig. 15). Following the vertical profiling, azimuthal Wenner-Lee surveys were conducted in the following way. The Wenner-Lee array was set up and the azimuth of the line recorded (N4°E). Current, potential, and SP were recorded for the three electrode spacings (7.62, 10.67, and 15.24 m). The array was then rotated about its fixed midpoint by 10° (to N14°E). The current and potential measurements were then made at each of the electrode spacings. The procedure

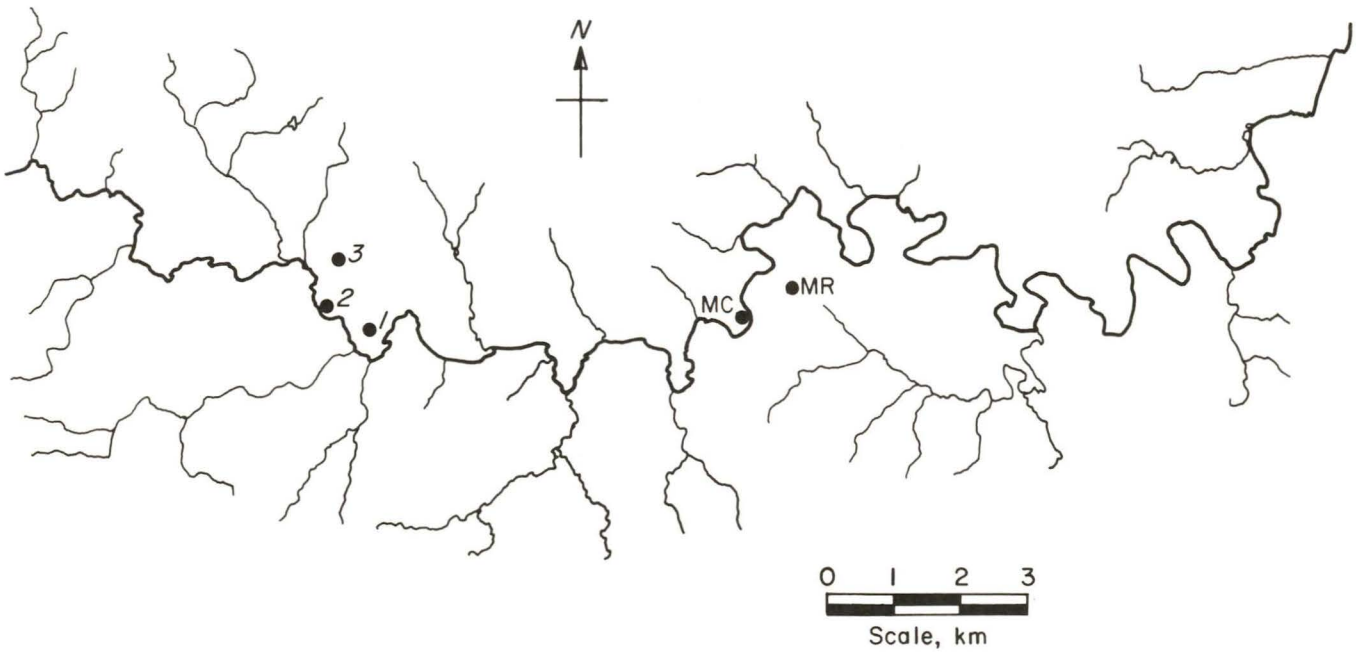


FIGURE 14. - Portion of drainage map of South Branch, Root River, including Spring Valley, Mystery Ridge, and Mystery Cave study areas.

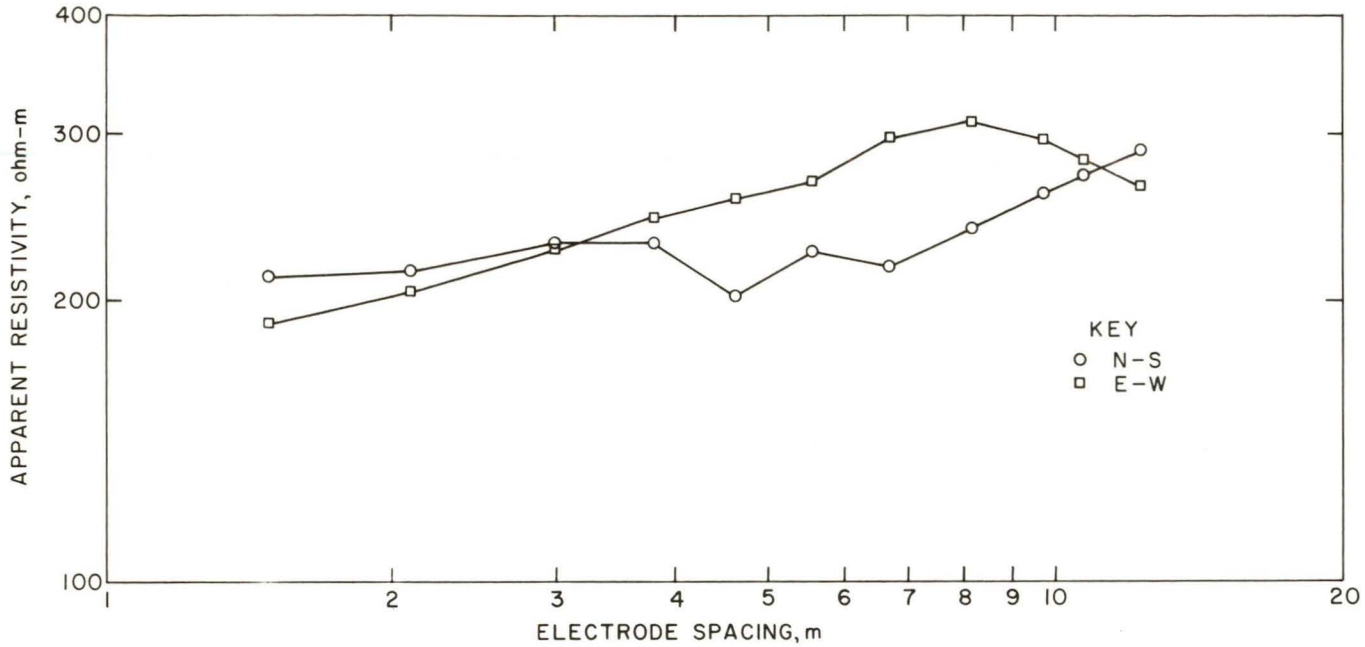


FIGURE 15. - Perpendicular, vertical profiles, site 1, Spring Valley study area, early spring 1982.

was repeated until the array had been rotated through an arc of 180°. Increments of less than 10° were found to be too time consuming for the purposes of this study, while increments of 20° or more provided only sketchy data. This field procedure was followed throughout the study.

Azimuthal Wenner-Lee surveys were conducted at sites 1 and 2 in March and at site 3 in May; a horizontal profile across the field at site 2 was also conducted in May. All electrical measurements in the studies were made with a Bison signal enhancement resistivity system (2390).

Results

Azimuthal survey data are presented as Wenner graphs and as Lee graphs. The Wenner graphs (prepared from the normal readings on the instrument) and the Lee graphs (from the Lee-left and Lee-right readings) are sets of graphs presenting data from all electrode spacings at a particular site. Notice that the Wenner graphs must always be symmetrical because the survey data from 0° to 180° are merely repeated from 180° to 360° to complete the graph. Lee graphs can be and usually are asymmetrical because as the survey is run, separate measurements of apparent resistivity are made on each side of the array. The apparent resistivities on either side of the array will vary slightly due to local inhomogeneity, structure, or topography.

Azimuthal Survey, Site 1

The Wenner survey results for site 1 (figure 16*A* and table 4) indicate that the theory of resistivity anisotropy holds for jointed rocks, since there is an apparent resistivity maximum associated with each of the three known joint sets found in the study area. This result is different from the expected result, which was that an apparent resistivity maximum would be associated with the predominant joint set only. Another unexpected feature shown in figure 16*A* is that the character of the graphs vary significantly. At the electrode spacing equal to 7.62 m, the graph is approximately elliptical, with $\lambda = 1.11$; at 10.67 m, the graph is nearly circular; at 15.24 m, the graph has two apparent resistivity maxima.

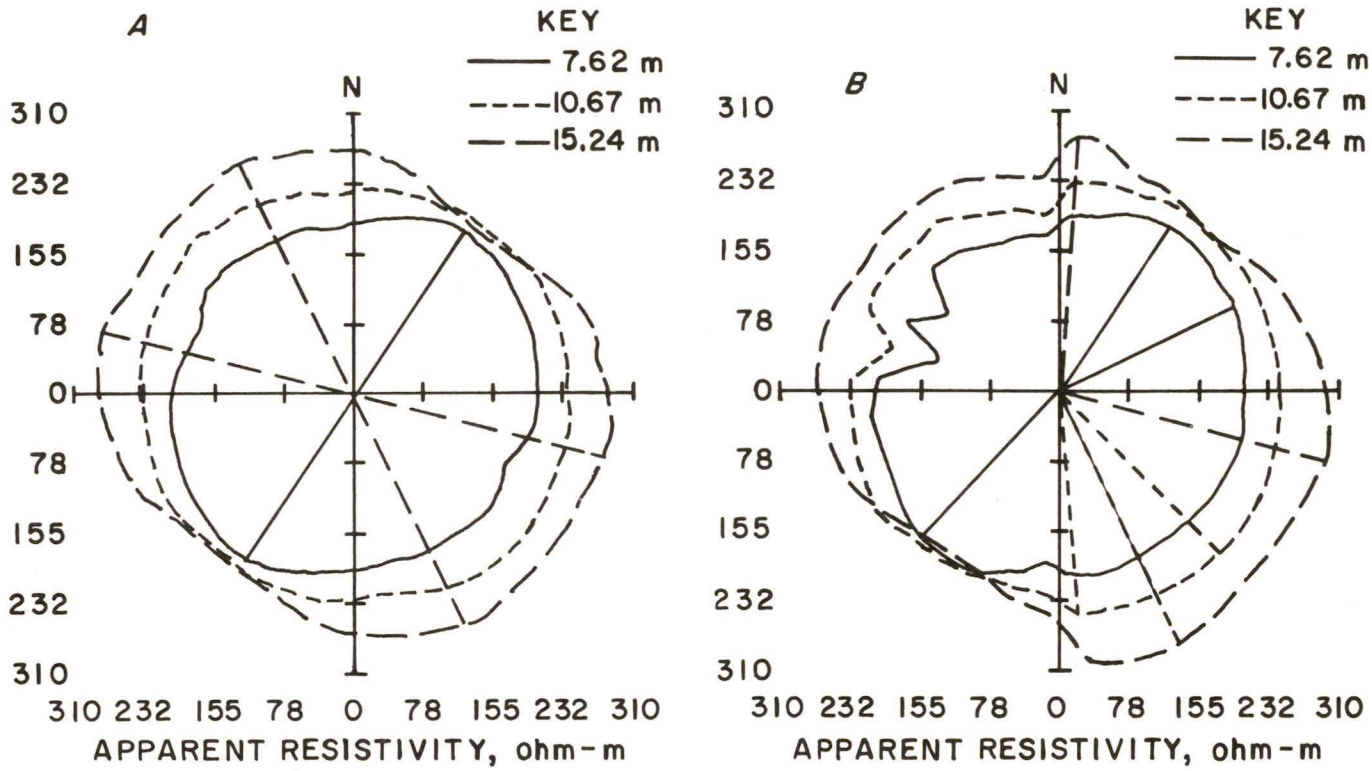


FIGURE 16. - Wenner (*A*) and Lee (*B*) apparent resistivity graphs from azimuthal Wenner-Lee surveys, site 1, Spring Valley study area, Minnesota.

The Lee graphs (fig. 16*B*) are similar to the Wenner graphs but with two additional features. The graphs are asymmetrical and more irregular, with numerous apparent resistivity peaks (table 4). The asymmetry, which occurs at all electrode spacings, may be due to local structure, such as a slight dip to the WNW direction. This interpretation is supported by the direction of the slope of the water table observed in bedrock monitoring wells at the landfill.

TABLE 4. - Azimuths of relative maximum apparent resistivity, Spring Valley, site 1, degrees

Electrode spacing...m..	7.62	10.67	15.24
Wenner.....	34	NAp	104
	214	NAp	154
	NAp	NAp	284
	NAp	NAp	334
Lee.....	34	134	4
	64	154	104
	224	174	154

NAp Not applicable.

Azimuthal Survey, Site 2

The survey at site 2 was run on the same day as the site 1 survey; the measurement interval was increased to 15° in order to complete the rotation in the time available. At site 2, there is an apparent resistivity maximum in the NE-SW direction (figure 17 and table 5). The potential readings were, however, very unstable. (The battery was checked in the field and was not the source of the problems.) In the E-W direction the instability was even greater; in some cases, no readings of potential or SP could be made. During the return trip, made in the spring, a horizontal profile was conducted across the field at site 2 in order to determine the extent of the anomalous zone. The apparent resistivities changed significantly along the length of the horizontal profile, although the field was nearly flat and bedrock was flat-lying to slightly dipping (fig. 18). The changes in apparent resistivity probably indicate topographic relief on the upper bedrock surface in

this area of active karstification. Bedrock was observed near the surface at the north end of the profile, between stations 60 and 70.

TABLE 5. - Azimuths of relative maximum apparent resistivity, Spring Valley, site 2, degrees

Electrode spacing...m..	7.62	10.67	15.24
Wenner.....	14	14	54
	194	54	234
	NAp	84	NAp
	NAp	194	NAp
	NAp	234	NAp

NAp Not applicable.

Azimuthal Survey, Site 3

Wenner and Lee graphs for site 3 (figure 19 and table 6) show good agreement with the graphs from site 1 in the directions of the apparent resistivity maxima, the coefficients of anisotropy, and in the asymmetry of the Lee graphs. At the smaller electrode spacings, the Wenner apparent resistivity graphs are elongated

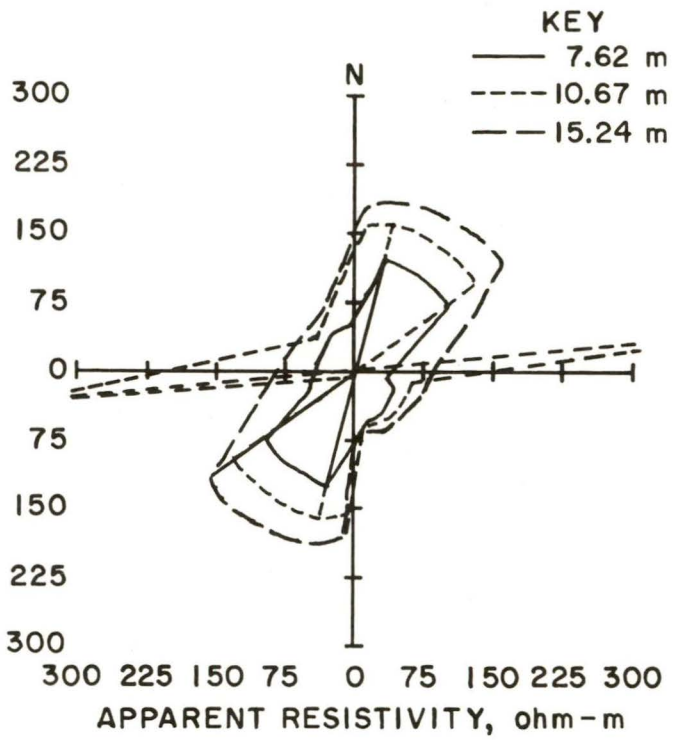


FIGURE 17. - Wenner apparent resistivity graphs from azimuthal Wenner-Lee surveys, site 2, Spring Valley study area, Minnesota.

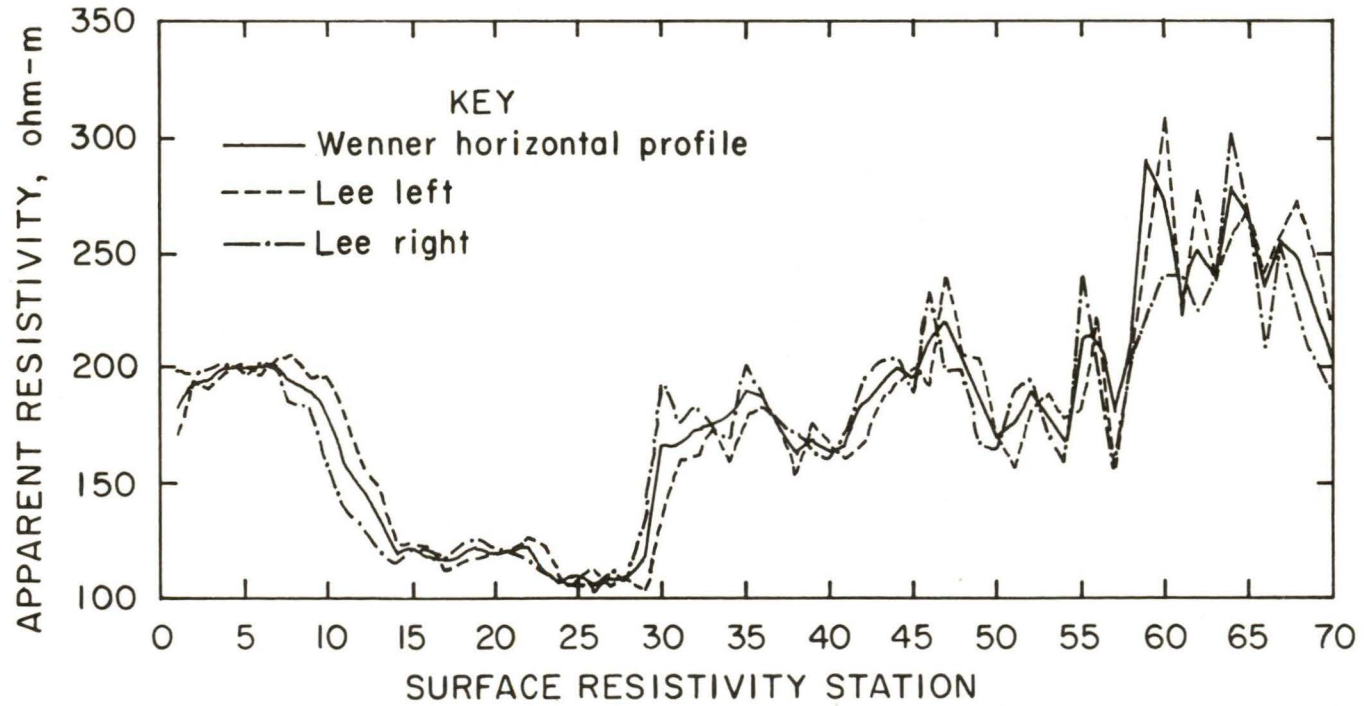


FIGURE 18. - Horizontal profile, site 2, Spring Valley study area, Minnesota; resistivity station 1 is at south end of field.

in the NE-SW direction; at the largest electrode spacing, the apparent resistivity graph is elongated in the NW-SE direction. The coefficients of anisotropy are 1.07, 1.11, and 1.03 for electrode spacings of 10.67, 15.24, and 22.86 m, respectively. The Lee graphs show a high resistivity in the southeast quadrant.

TABLE 6. - Azimuths of relative maximum apparent resistivity, Spring Valley, site 3, degrees

Electrode spacing.....m..	7.62	10.67	15.24	22.86
Wenner.....	NAp	54	44	154
	NAp	234	224	334
Lee.....	24	54	44	64
	94	94	104	134
	114	114	164	164
	NAp	154	214	NAp
	NAp	204	NAp	NAp

NAp Not applicable.

There are also significant differences between the site 1 and site 3 survey results as well. The differences shown in the graphs probably result from seasonal differences at the sites, in particular the presence of the frost layer at site 1 during the winter survey. The frost layer would affect both the depth of penetration for a given electrode spacing and the magnitude of apparent resistivity at the smaller electrode spacings. (The additional electrode spacing, 22.86 m, was run at site 3 in anticipation of these effects.)

The Wenner graph for 7.62 m (fig. 19*A*) shows little elongation and is probably most affected by the true resistivity of the unjointed soil layer. The graphs for electrode spacings of 10.67 and 15.24 m at site 3 are similar in shape to Wenner graphs for the electrode spacing of 7.62 m at site 1 (fig. 16*A*). The coefficients

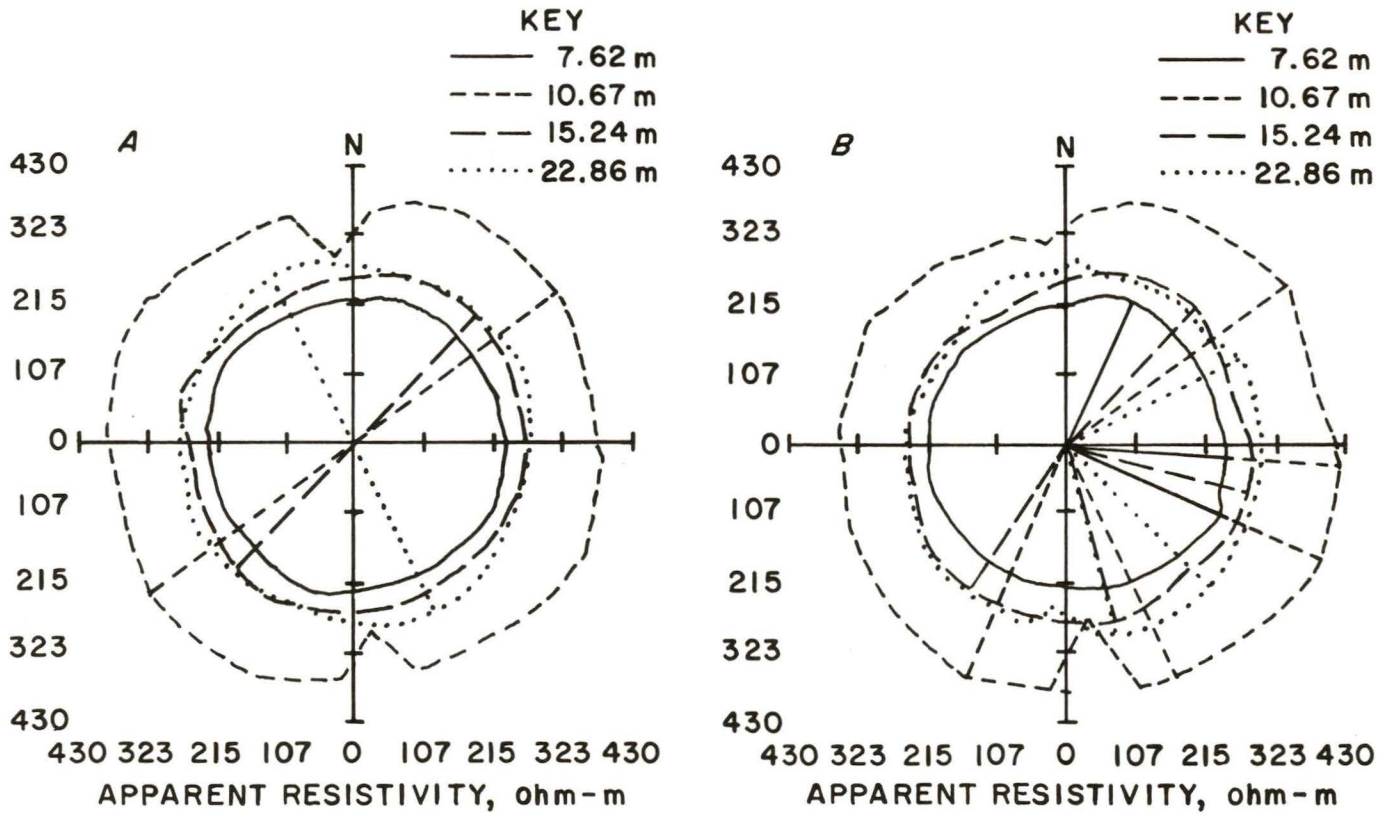


FIGURE 19. - Wenner (*A*) and Lee (*B*) apparent resistivity graphs from azimuthal Wenner-Lee surveys, site 3, Spring Valley study area, Minnesota.

of anisotropy are also very similar. For the electrode spacings of 22.86 m at site 3, there is a NW-SE elongation. It is surprising that there is no apparent resistivity maximum in the E-W direction at any electrode spacing at site 3, although the E-W joint set was thought to be predominant in the study area. SP's measured at sites 1 and 3 do not show any obvious trends (figs. 20-21).

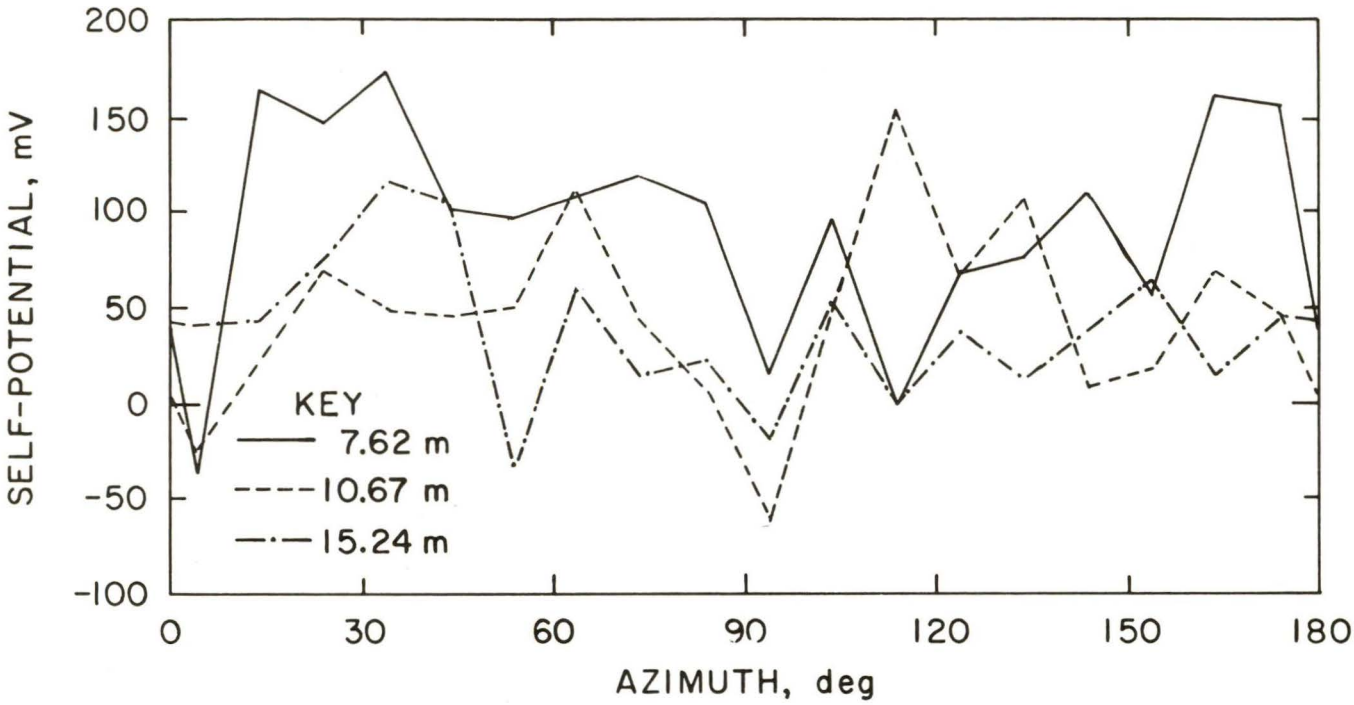


FIGURE 20. - Self-potential, azimuthal survey, site 1, Spring Valley study area, Minnesota.

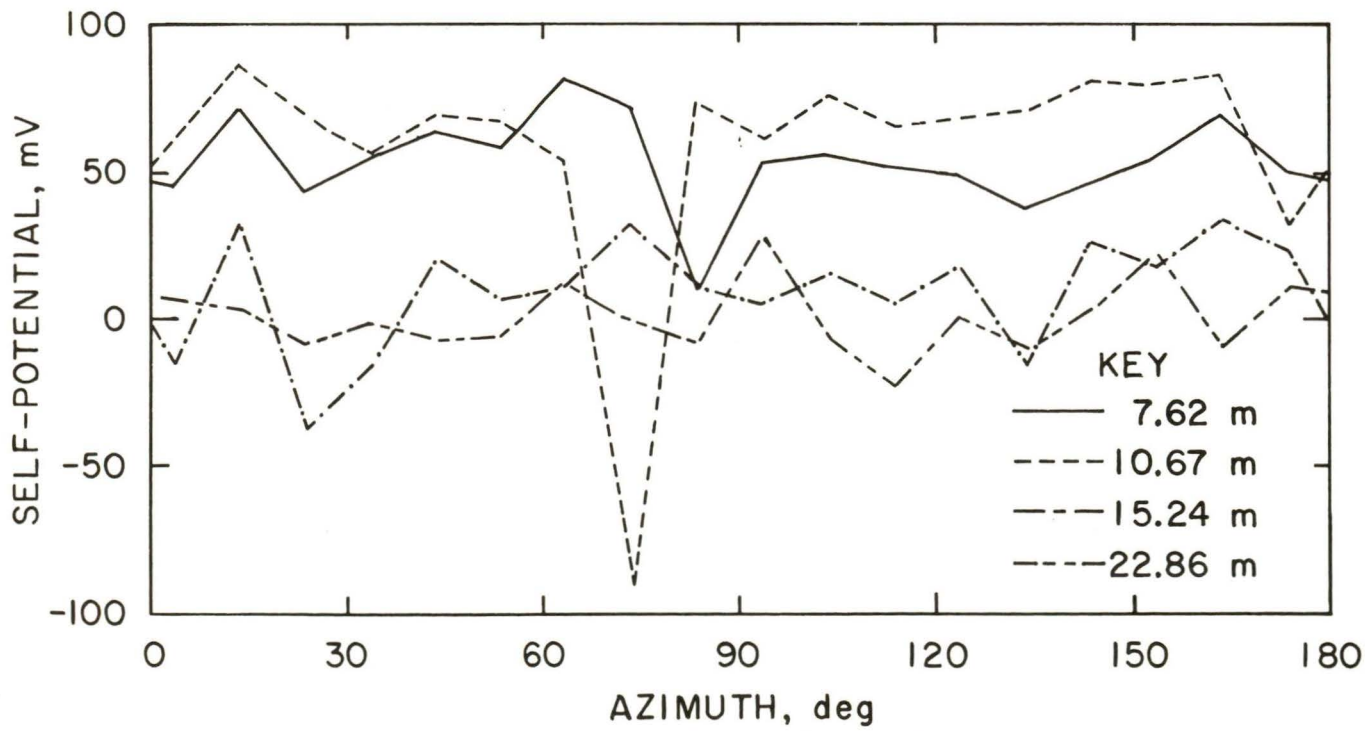


FIGURE 21. - Self-potential, azimuthal survey, site 3, Spring Valley study area, Minnesota.

Conclusions

At Spring Valley sites 1 and 3, the azimuthal surveys produced elliptical apparent resistivity graphs having the major axis in the direction of the strike of a joint set present at the study area. Therefore, the theory of resistivity anisotropy applies to at least some jointed formations. Nonelliptical graphs, both circular graphs and graphs having more than one apparent resistivity peak, were also produced. These results cannot be adequately explained at this time.

The coefficients of anisotropy determined from the Spring Valley graphs are higher than the values from the physical model. This is a reasonable result, according to equation 24, since the true rock resistivity should be significantly higher than the true resistivity of the board matrix.

Graphs from azimuthal Lee surveys at sites 1 and 3 are consistently asymmetric, and this asymmetry may be related to structure (dip) or soil thickness. Available data are not sufficient to draw a firm conclusion.

The source of the measurement problem at site 2 was not determined in the study, in part because the work would require many hours in the field for additional horizontal profiling. This brings up one disadvantage with the surface resistivity methods: even under ideal conditions the work requires a great deal of time and produces relatively little data compared with other geophysical methods.

SHANNOPIN MINE, GREENE COUNTY, PA

Description of Study Area

The Shannopin Mine is an underground coal mine located in Greene County in southwestern Pennsylvania (fig. 22). The Pittsburgh coal seam is mined at Shannopin; the minable thickness is about 2 m. The mine was developed on the flank of a syncline where the dip of bedrock is to the northwest at approximately 2°. Table 7 describes the stratigraphy of the Pittsburgh Formation. Strata overlying the coalbed and roof shale vary in the study area from interbedded sequences of limestone, shale, and siltstone, to shale and sandstone (23). The strike directions of both coal cleat and surface joints have been measured at the Shannopin Mine (table 8). Superimposed on the naturally occurring joints, particularly in areas that have been retreat mined, are subsidence fractures that were expected to be the predominant fractures in the study area.

Much of the subsurface has been dewatered after years of mining, although wet zones occur in some sections of the mine. In a separate Bureau investigation at the Shannopin Mine, zones of substantial mine water infiltration had been delineated. One of the wet areas of the mine was located under a narrow river valley, and it seemed likely that stream flow was

TABLE 7. - General geology, Shannopin Mine, Greene County, PA (23)

Depth, m	Formation and description
0 to 24.....	Upper Member Pittsburgh Formation; includes 4 limestone units separated by shale or sandy shale beds.
24 to 52....	Sewickley Member, Pittsburgh Formation; thick limestone sequence with the Sewickley coalbed at its base.
52 to 56....	Fishpot Member, Pittsburgh Formation; siltstone and mudstone.
56 to 69....	Redstone Member, Pittsburgh Formation; siltstone and mudstone overlain by a relatively persistent limestone; the Redstone Coalbed is at its base.
69 to 88....	Lower Member, Pittsburgh Formation; includes the Pittsburgh Coalbed at the base, Pittsburgh sandstone may be present and/or sandy shale.

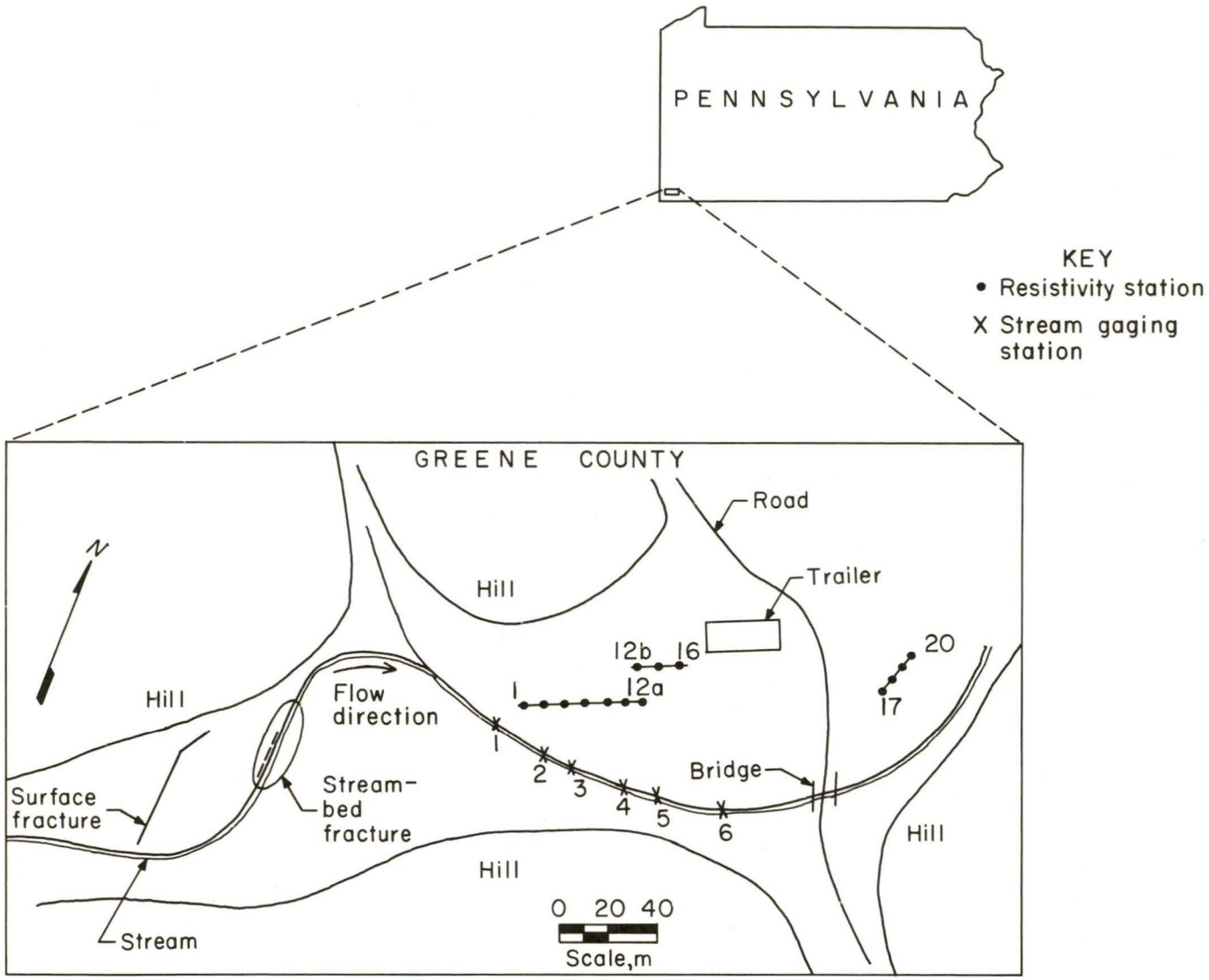


FIGURE 22. - Site map and index map, Shannopin Mine, Greene County, PA.

TABLE 8. - Average strike of joints and coal cleat, Shannopin Mine, Greene County, PA (23)

Structural feature	Strike
Face cleat (predominant joint in coal).	N73°W.
Butt cleat.....	N18°E.
Surface joints.....	N80°W, N23°E.

diverted to the mine through joints or fractures in the streambed. Stream gaging, however, gave inconclusive results, and zones of water loss from the stream could not be located with confidence. Because treatment of the entire stream by channelization or grouting would be far too expensive, the electrical methods under development were used at the Shannopin Mine in an attempt to locate zones of increased jointing and/or fracturing that provided flow paths from the surface to the mine. At the same time, the basic hypothesis of the study was tested.

The field site selected is in a narrow valley, approximately 30 to 40 m wide (fig. 22). The valley walls are steep and approximately 30 m high. The depth to the Pittsburgh seam beneath the valley floor is approximately 60 m. Joints could be seen in bedrock in some sections of the streambed. The measured

orientations are given in table 9. It was essential to measure the exposed joints in the streambed even though they were few in number, because the published joint information applies to the entire mine, a large area of complex stratigraphy with local variations in structure.

TABLE 9. - Strike of joints and fractures at field site, Shannopin Mine, Greene County, PA

Structural feature	Strike
Joints in streambed (in order of number of joints measured).	N31°E, N17°E, N68°E, N36°W, N81°W.
Subsidence fractures.....	N10°E.

Description of Fieldwork

The Shannopin field study was conducted as follows. First, soundings were done parallel with and then perpendicular to the valley walls to determine the maximum electrode spacing that could be used in the surveys without getting topographic effects. Then azimuthal surveys were run in order to test the method for determining joint strike. The results of the survey were compared with the published joint strike data and with the strike of subsidence fractures and the joint strike directions measured in bedrock in the stream bed at the site. SP's were also measured in the azimuthal surveys. Finally, a horizontal profile was run down the length of the valley, maintaining a constant array orientation, in order to locate zones of low apparent resistivity. Low resistivity would indicate zones of intense jointing or fracturing, which would permit water to flow to the mine.

Results

Azimuthal Wenner and Lee surveys were conducted at an upstream site (station 1), and at a site about midway down the valley (station 12a). The center of the array was positioned approximately midway between the valley walls. An electrode spacing of 6.10 m and a measurement interval was 10° were used throughout the survey.

The graphs from both stations are approximately elliptical (figure 23 and table 10). The N-S maximum apparent resistivity agrees well with the strike of large subsidence fractures visible at the site. The NW-SE peak corresponds to the strike of one of the most frequently occurring joint sets measured in the streambed. The apparent resistivity maxima do not agree well with average joint strike for the entire mine, however. The coefficients of anisotropy calculated from the Wenner graphs are 1.47 at station 1 and 1.32 at station 12a, both of which are higher than any of the coefficients of anisotropy from the Spring Valley sites.

Azimuthal Surveys

The Lee survey results are asymmetrical, with the high apparent resistivities occurring in the southeastern quadrant. This direction agrees with the dip of the bedrock at the minesite. Although changes in the soil thickness could reasonably account for the asymmetry, the soil visible at the stream bank from station 1 to station 20, appeared to be uniform in thickness.

SP's measured in the azimuthal Wenner configuration are shown in figure 24. The most prominent feature of the data is the drop in potential between approximately N120° to 160°E at station 12a. This direction agrees with the joint direction measured directly in the bedrock exposed in the streambed and with the direction of an apparent resistivity maximum in the azimuthal survey at station 12a. This drop in naturally occurring potential along a known joint strike is thought to be the streaming potential, resulting from flow of ground water through the joint set at station 12a. A significant, though smaller, drop in potential occurs at station 12a at N10° to 30°E, which corresponds fairly well to the observed strike of subsidence fractures and to the maximum apparent resistivity at that station.

TABLE 10. - Azimuths of relative maximum apparent resistivity, Shannopin Mine, degrees

(6.10-m electrode spacing)

Station	1	12a
Wenner	179	149
	359	179
	NAp	329
	NAp	359
Lee	119	89
	149	179
	179	329
	359	NAp

NAp Not applicable.

Horizontal Profile

A horizontal profile was conducted down the center of the valley (fig. 25). The profile was interrupted between stations 16 and 17 because a house, road, and bridge blocked the path. The profile was continued on the opposite side of the road. The electrode spacing used was 6.10 m at a resistivity station spacing of 3.05 meters. The Wenner-Lee array was used in the profiling.

The orientation of the resistivity array was kept constant throughout the profiling. This is important for carrying out a survey of this type in jointed rock. The range in apparent resistivity values due to orientation of the array alone is from 238 to 147 ohm-m at station 1 (Wenner array). This is a drop of 38 pct. The drop in apparent resistivity due to increased jointing or fracturing was expected to be on that order of magnitude. Therefore, the array must be kept at a constant orientation, even when the orientation of the valley changes, in order to delineate zones of low resistivity due to changing joint-fracture intensity.

The apparent resistivities decrease by more than 50 pct from the upstream station beyond station 12. Across the river, apparent resistivities increase again. An interesting feature of the data is that from stations 1 to 16 the curves for the Lee-right, Wenner, and Lee-left measurements are offset. At stations 17 to 20 this offset is not present. This is thought to be due to the fact that at stations 1 to 16, the

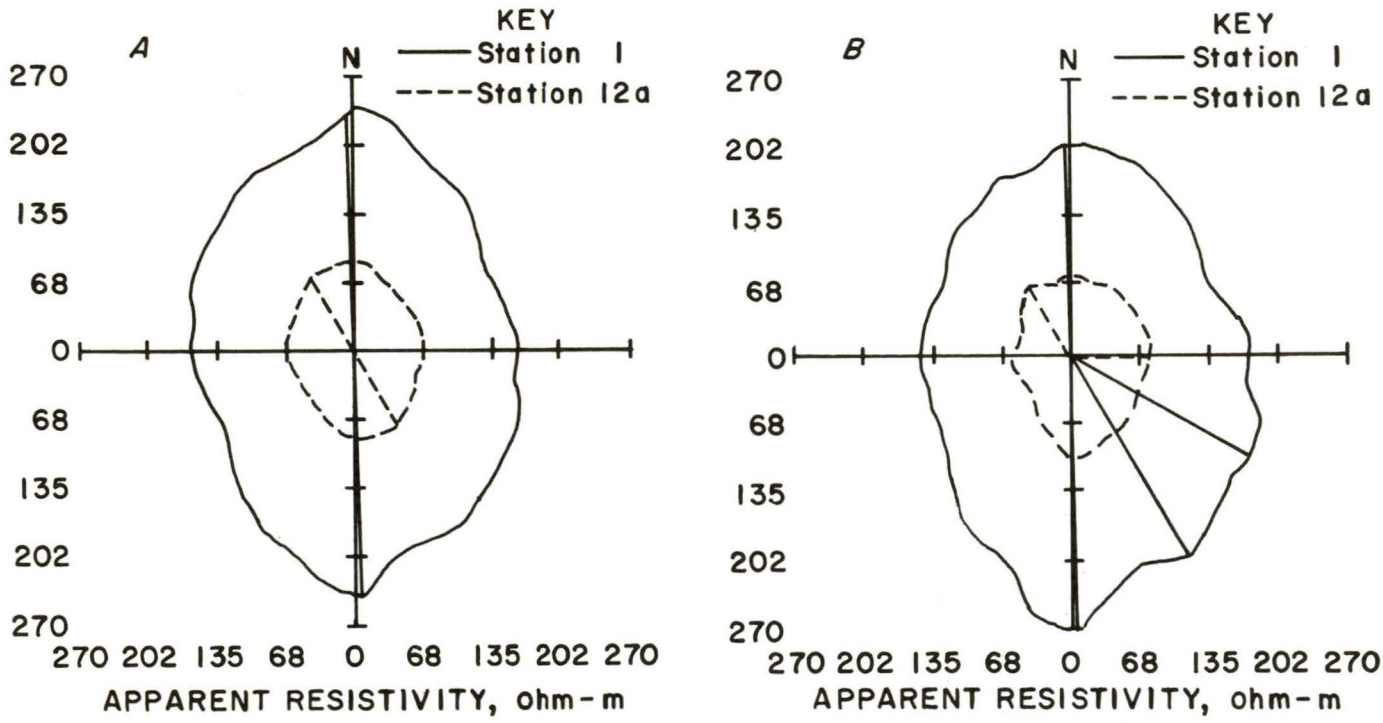


FIGURE 23. - Wenner (*A*) and Lee (*B*) apparent resistivity graphs from azimuthal Wenner-Lee surveys, Shannopin Mine, Greene County, PA.

entire array was set up with the Lee-right electrode leading and the Lee-left electrode following as the survey moved down valley; at stations 17 to 20, the entire array was being moved away from the zone of low apparent resistivity in a parallel movement.

Approximately 2 weeks after the electrical measurements were completed, stream flow was measured at stations H1 to H6. Flow was very low at that time, making measurement difficult. During low flow, however, the amount of water lost through joints or fractures is a larger

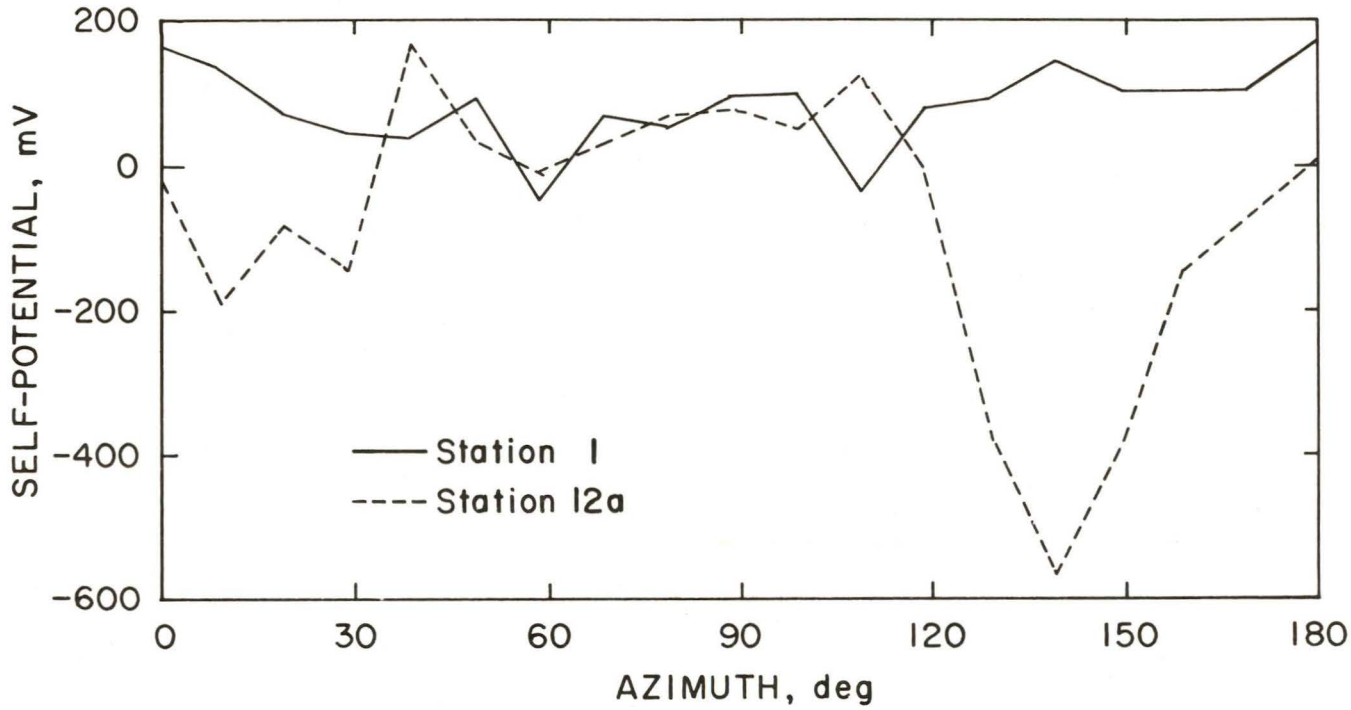


FIGURE 24. - Self-potential azimuthal surveys, stations 1 and 12a, Shannopin Mine, Greene County, PA.

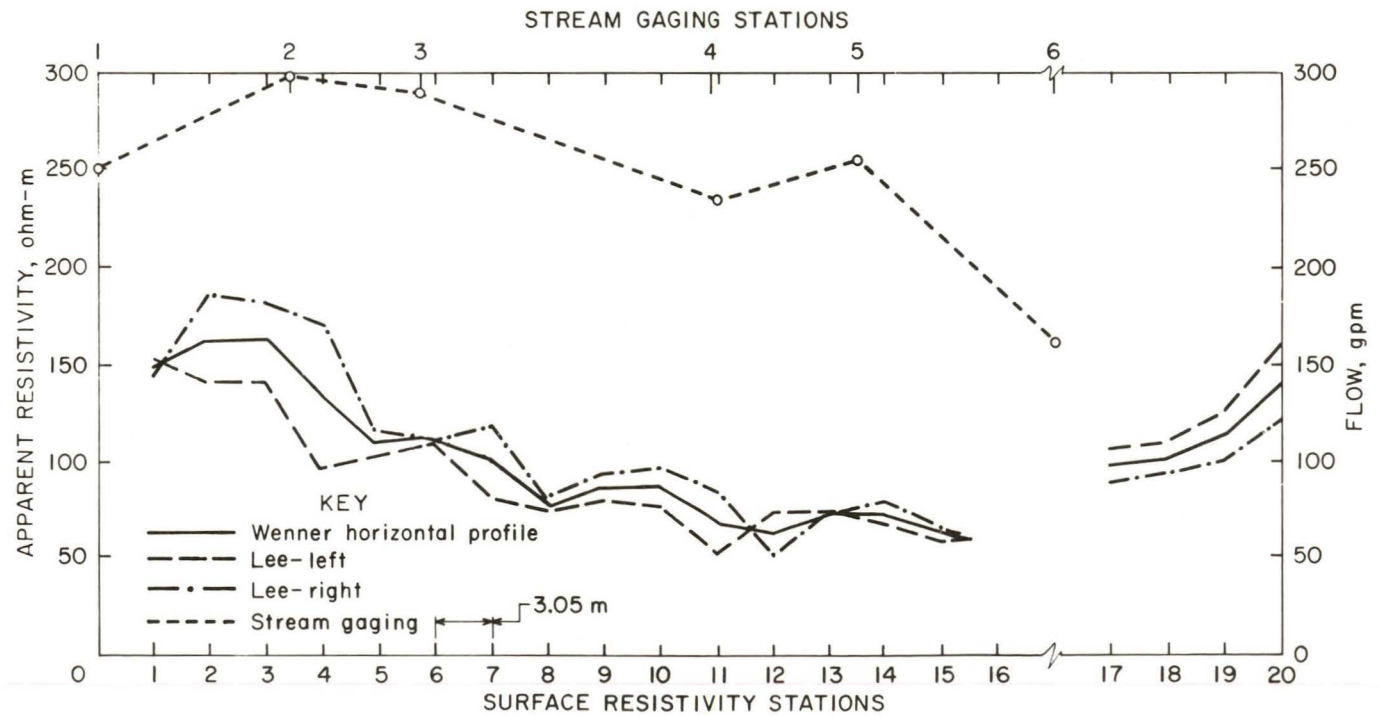


FIGURE 25. - Horizontal profile and stream gaging results, Shannopin Mine, Greene County, PA.

portion of the total flow than during high flow, and the chances of having a measurable drop in flow across a jointed or fractured zone are enhanced. The results of the stream gaging are given in figure 25. Stream flow losses correspond well with the drop in apparent resistivity. Several days after the stream gaging was completed, mining upstream from the site caused additional subsidence fracturing. As a result, the entire stream was diverted into the mine.

Conclusions

At the Shannopin Mine site, there was good agreement between the strike of subsidence fractures and the direction of the maximum apparent resistivity measured in azimuthal surveys, although the effect of joints was much less obvious. The apparent resistivity graphs were approximately elliptical, with coefficients of anisotropy greater than those for the Spring Valley sites or the model study. There are a number of factors that could cause higher coefficients of anisotropy (according to equation 24). At a mined site such as this, both increased joint and fracture frequency and increased joint and fracture width seem to be likely. The azimuthal survey, horizontal profiling, and SP methods were tested in a practical mining situation and were found to be useful. The results of the SP survey were especially encouraging and support earlier reports of SP being used successfully to locate zones of ground water inflow.

The Shannopin Mine study demonstrated not only the usefulness of electrical methods, but also the care that must be taken to avoid problems imposed by topography and structure. The study also indicated the need for additional field data. The interpretation of the resistivity and SP data was limited by the lack of information about fracture and joint width, spacing, filling, and the degree of saturation at the site. Finally, although the resistivity method was very time consuming, the method is faster and provides more information than stream gaging.

NEDA AND BEECHWOOD SITES, DODGE COUNTY, WI

Site Description and Summary of Site Characteristics

The southeastern Wisconsin study area includes the Neda and Beechwood field sites in Dodge County (fig. 26). The geology of the sites is summarized in table 11. At both of the sites, the oldest formation of interest is the Maquoketa

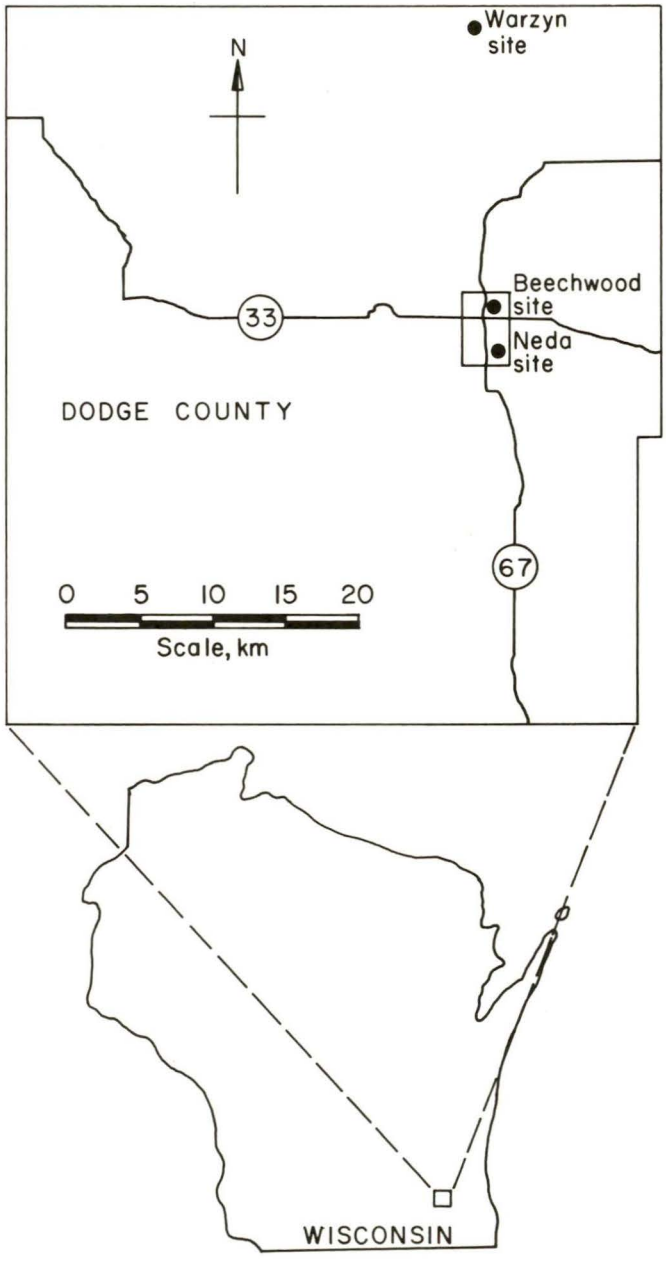


FIGURE 26. - Index map and site map, Neda and Beechwood sites, Dodge County, WI.

TABLE 11. - General geology, Neda and Beechwood sites, Dodge County, WI (1)

Depth, m	Formation and/or description
Neda:	
0 to 1.52.....	Quaternary glacial deposits, mostly clay.
1.52 to 16.76.	Niagran Dolomite, Mayville Member (Silurian); thick-bedded, uneven-textured dolomite; light gray to light brown on weathered surface, highly resistant; may contain less resistant sand lenses; vuggy in some places.
16.76 to 19.81	Neda Formation (Ordovician); oolitic iron ore, reddish brown in color; thickness is variable; some beds of iron oxides with no oolites.
Below 19.81...	Maquoketa Shale (Ordovician); thin-bedded, green to brown, fossiliferrous shale with interbedded nodular limestones and thin-bedded dolomitic limestones; thickness approximately 60 m.
Beechwood:	
0 to 3.05.....	Quaternary glacial deposits.
3.05 to 33.53.	Niagran Dolomite, Mayville Member (Silurian); thick-bedded, uneven-textured dolomite; light gray to light brown on weathered surface; highly resistant; vuggy in some places.
Below 33.53...	Maquoketa Shale (Ordovician); thin-bedded, green to brown, fossiliferrous shale with interbedded nodular limestones and thin-bedded dolomitic limestones; highly weathered.

Formation (Ordovician), a shale with interbedded limestone having a thickness of about 70 m in the study area. Overlying the Maquoketa unconformably is the Neda Iron Formation (Upper Ordovician-Lower Silurian), a limestone consisting of oolites coated with iron oxides. The Neda Formation does not appear to be present at the Beechwood site. The formation at the study area is the (Silurian) Niagran Dolomite. The Niagran Formation forms an escarpment that is a prominent physiographic feature in eastern Wisconsin. Bedrock in the area dips slightly to the east and forms a part of the Michigan Basin. The dolomite has an upper highly weathered zone over an unweathered layer. A clay-rich layer of Pleistocene glacial material overlies the Niagran Dolomite. Except for the escarpment, topography in the area is relatively flat. The water table at both of the sites is near the top of the Maquoketa Formation; numerous springs occur along the escarpment.

The Neda Iron Formation was mined from about the mid-1800's until 1928. Production stopped because the high sulfur and phosphorus content of the ore made it unsuitable for steel. Many mine adits and air vents can be found at the Neda site. A mine map (fig. 27) shows the

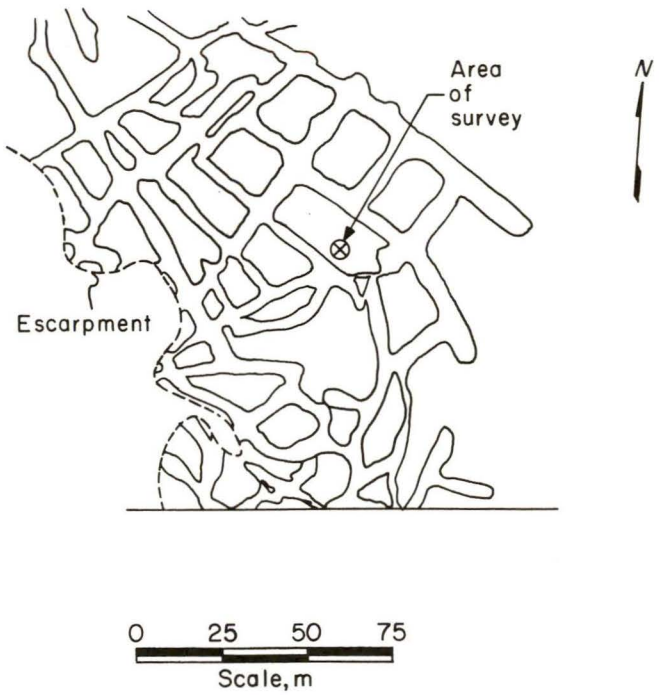


FIGURE 27. - Map of iron ore mine at Neda site, Dodge County, WI (2).

approximate position of the Neda site with respect to the mine voids. Extensive fracturing of the Niagran Dolomite because of blasting and mine subsidence was expected at Neda, and was expected to result in higher fracture porosity and permeability at the site. The Beechwood site is undeveloped, with numerous glacial erratics and large beechwood trees present. The Niagran Dolomite was expected to be jointed but not otherwise fractured.

The Wisconsin study area had the advantages of a nearby escarpment for conducting a joint survey, as well as having both mined and unmined sites of nearly the same geology. The deep water table found at both sites turned out to be a disadvantage, however, since the effect of changing moisture conditions in the vadose zone upon the resistivity was significant but not anticipated at the beginning of the study.

The field investigation at Neda and Beechwood was conducted by the University of Wisconcin-Milwaukee under a contract with the Bureau. It included an evaluation of azimuthal seismic velocity and attenuation methods for detecting joints and an evaluation of a permanently installed monitoring array, as well as the azimuthal resistivity study reported here (2).

The soil depth and thickness of the weathered dolomite were about the same and the dolomite was unsaturated at both sites. The average strike of the joint sets at the sites were nearly the same, with joints at N44°E and N133°E at Beechwood and at N44°E and N141°E at Neda, and standard deviations of 22°, 15°, 24°, and 20°, respectively.

Porosity and permeability were higher at Neda than at Beechwood. Seismic velocities of the unfractured cores at the two sites did not differ greatly, hence the bulk rock matrix is likely to be the same at both sites. From these results it can be argued that the joint width and/or frequency is greater at Neda than at Beechwood even though differences were not obvious at the escarpment adjacent to each site.

Preliminary Fieldwork

Joint orientations were measured with a Brunton-compass in unweathered Niagran Dolomite along the escarpment near both of the field sites. Approximately 1,000 measurements were made near the Neda site and approximately 300 were made near the Beechwood site where the escarpment was less accessible. The dip of the joints was generally 90° (vertical). Joint strike data are shown as rose diagrams in figures 28 and 29. The strike of lineaments measured on aerial photographs from 20 miles north of Neda are similar to joint strike at both of the field sites (fig. 30).

The joint survey results show two joint sets at right angles to one another in the study area. The NE-SW set occurs with slightly greater frequency according to the Neda and the Warzyn data. If random, mining-induced fracturing is present at Neda, it is not apparent from the joint data at the escarpment adjacent to the Neda site.

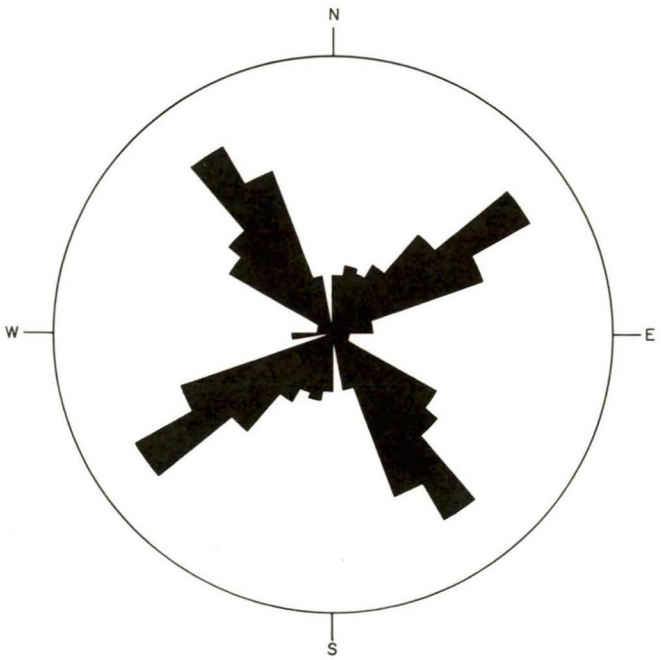


FIGURE 28. - Rose diagram of joint survey at Beechwood site, Dodge County, WI. Survey was done at escarpment; approximately 300 measurements taken (2).

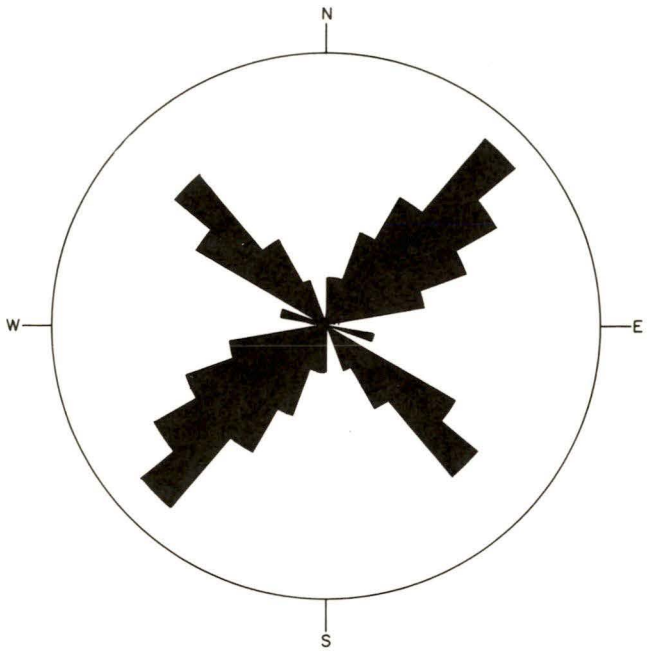


FIGURE 29. - Rose diagram of joint survey at Neda site, Dodge County, WI. Survey was done at escarpment; approximately 1,000 measurements taken (2).

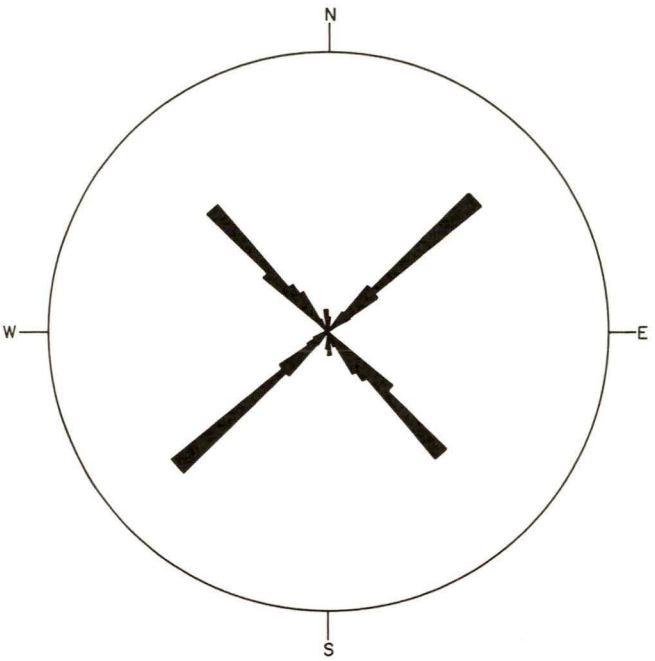


FIGURE 30. - Rose diagram of lineaments measured on aerial photographs, Warzyn site, Dodge County, WI (2).

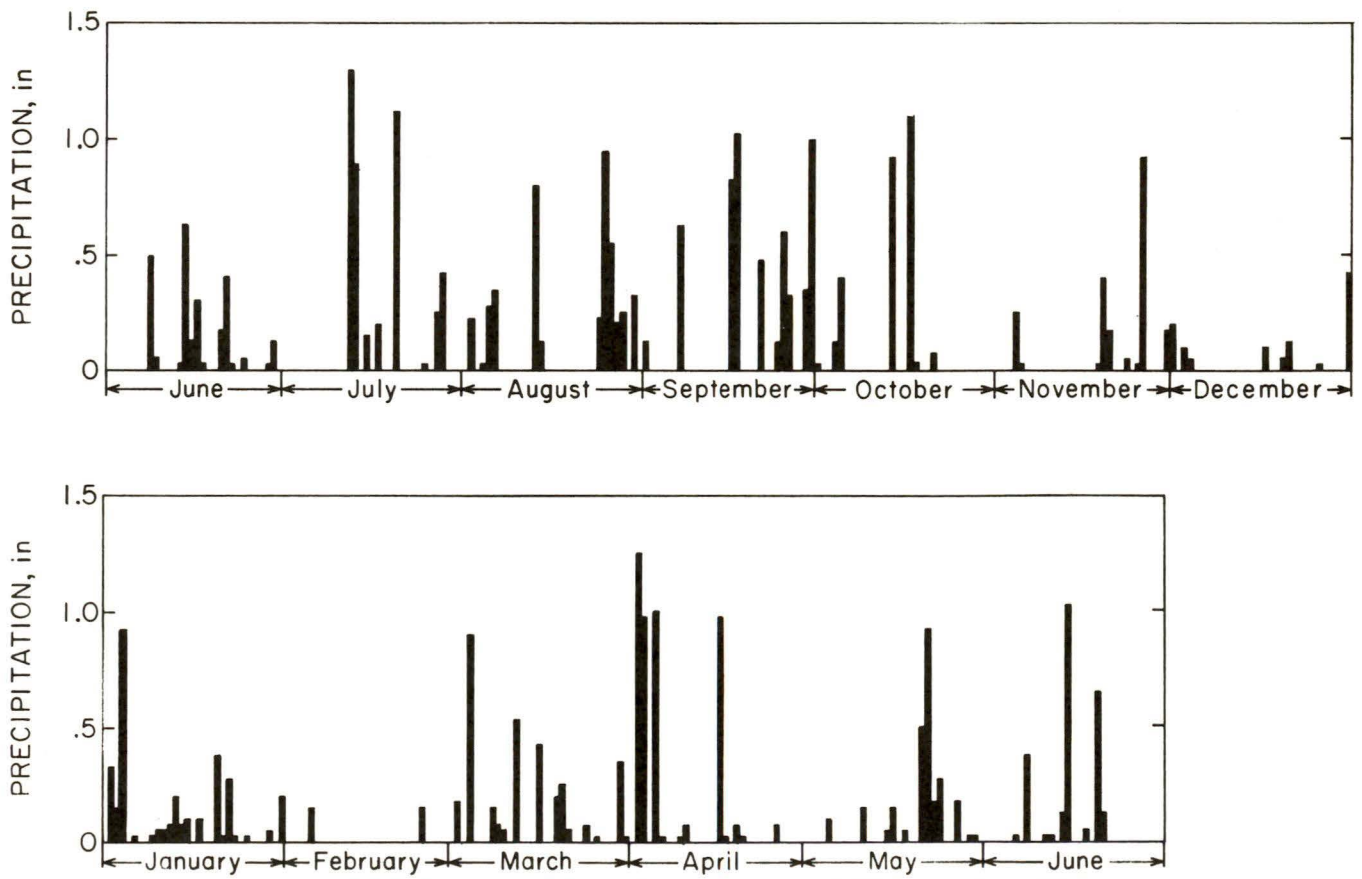


FIGURE 31. - Precipitation at West Bend, WI, 1981-82.

TABLE 12. - Porosity and permeability, Neda and Beechwood sites, Dodge County, WI (1)

Parameter	Neda	Beechwood
Porosity, ϕ, pct:		
From seismic data	4.1	1.32
From Bouguer density data	4-6	2-4
Permeability, K, from slug test, cm/s	0.03	0.011
Mean seismic velocity of unfractured rock core, m/s	[1]4,757.8	[2]5,711.1

[1]Average of 20 measurements. [2]Average of 7 measurements.

Standard geophysical methods were used to determine the bedrock porosity at the sites. The porosity measured by means of the gravity method is the average porosity of units above the Maquoketa Formation; the porosity determined from the seismic data is the porosity of the unweathered dolomite (table 12). Permeabilities were measured by slug tests in the weathered layer of the dolomite. The values are approximate; the weathered layer is so permeable that only with very large volumes of water could an accurate test be run. Since drilling fluid was lost in the weathered dolomite layer, additional slug tests in the unweathered zone were not attempted. The seismic velocities of unfractured cores from each site were measured in the laboratory. In addition to the geophysical data, precipitation records were available for the entire testing period from a station located 7 miles from the field sites (fig. 31).

Results

The electrode spacing needed to investigate the unweathered dolomite layer was determined at each site by measuring resistivity with various electrode spacings. Data were interpreted to determine depth to an interface between zones of different resistivities by master-curve matching (figs. 32-34).

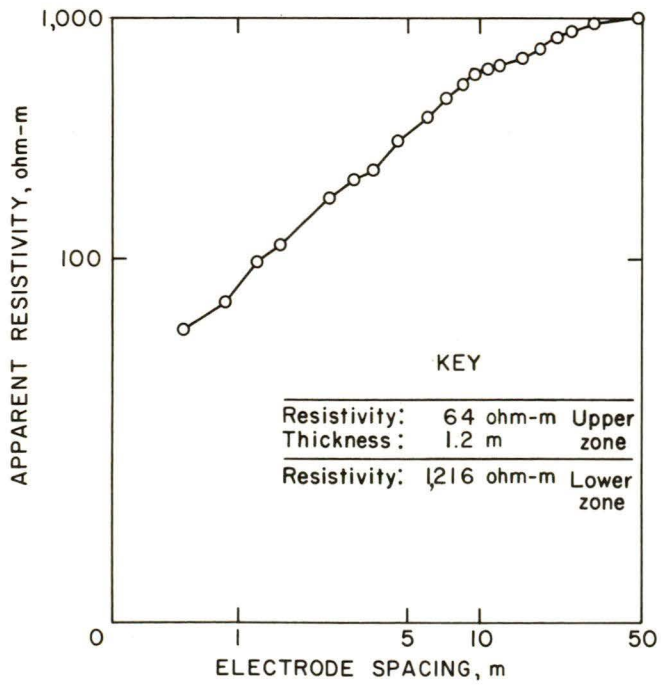


FIGURE 32. - Results of east-west depth sounding at Beechwood site. Interpretation by master-curve matching (2).

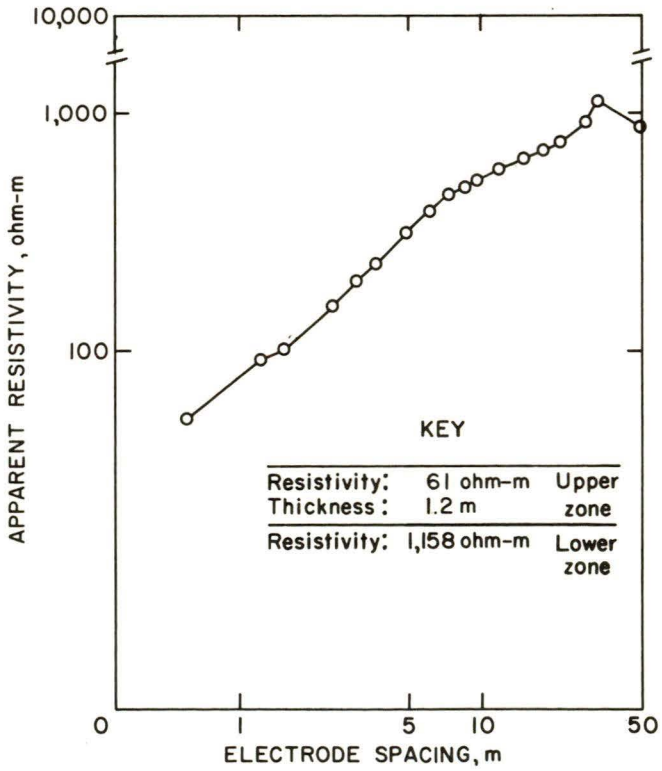


FIGURE 33. - Results from north-south depth sounding at Beechwood site using a Wenner array. Interpretation by master-curve matching (2).

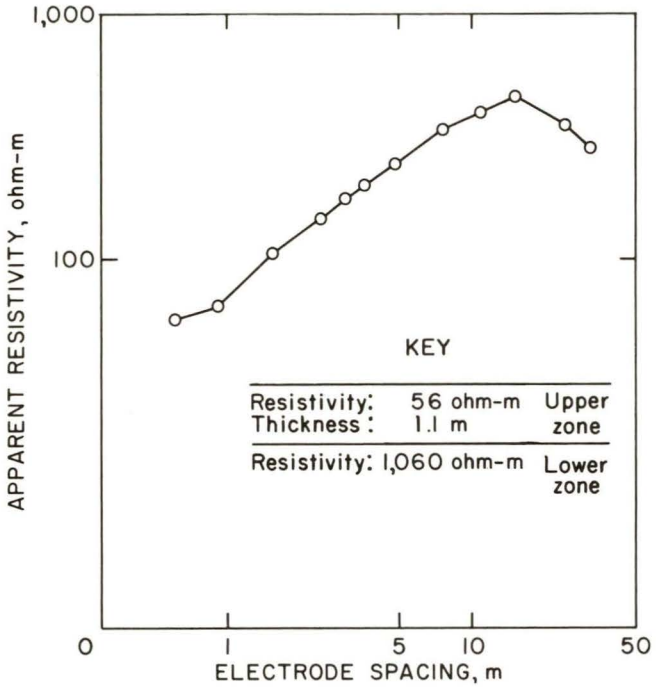


FIGURE 34. - Results from north-south depth sounding at Neda site using a Wenner array. Interpretation by master-curve matching (2).

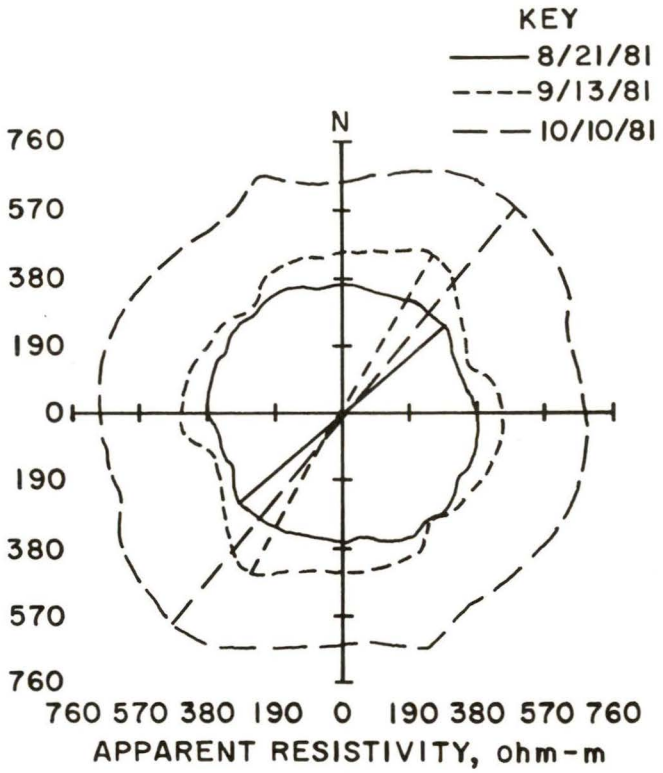


FIGURE 35. - Wenner apparent resistivity graphs from azimuthal Wenner surveys, Beechwood site, Wisconsin, fall 1981 (2).

With the electrode spacings selected to assure that the resistivity measured was primarily that of the unweathered dolomite, azimuthal Wenner and Wenner-Lee surveys were conducted at Beechwood and Neda during the late summer and fall of 1981 and the spring of 1982 (figs. 35-38). A 10° measurement interval was used in all of the surveys.

Three azimuthal Wenner surveys were run at the Beechwood site (figure 35 and table 13). The results show a change in both the azimuth of the maximum apparent resistivity and in the magnitude of the average apparent resistivity (shown by the size of the graph) over a 7-week period. The azimuth of the maximum apparent resistivity varied from N30°E to N50°E, a range that includes the average strike of a joint set measured at the escarpment (at N44°E) and which is within the ±22° standard deviation.

TABLE 13. - Azimuths of 1981 relative maximum apparent resistivity, Beechwood site, degrees

(13.62-m electrode spacing)

Date.....	8/21	9/31	10/10
Wenner.....	50	30	40
	230	210	220

A possible explanation for both of the observed changes is changing moisture conditions in the vadose zone. A drying out of the zone would result in an overall increase in resistivity as air replaces water in the voids. Differential drying out of joints according to width would also be expected, that is, "large" joints drying out before "small" joints and with "very small" joints retaining irreducible water indefinitely. Dry joints would be indistinguishable from bulk rock and would not be related to an apparent resistivity peak on the graph. The available precipitation data

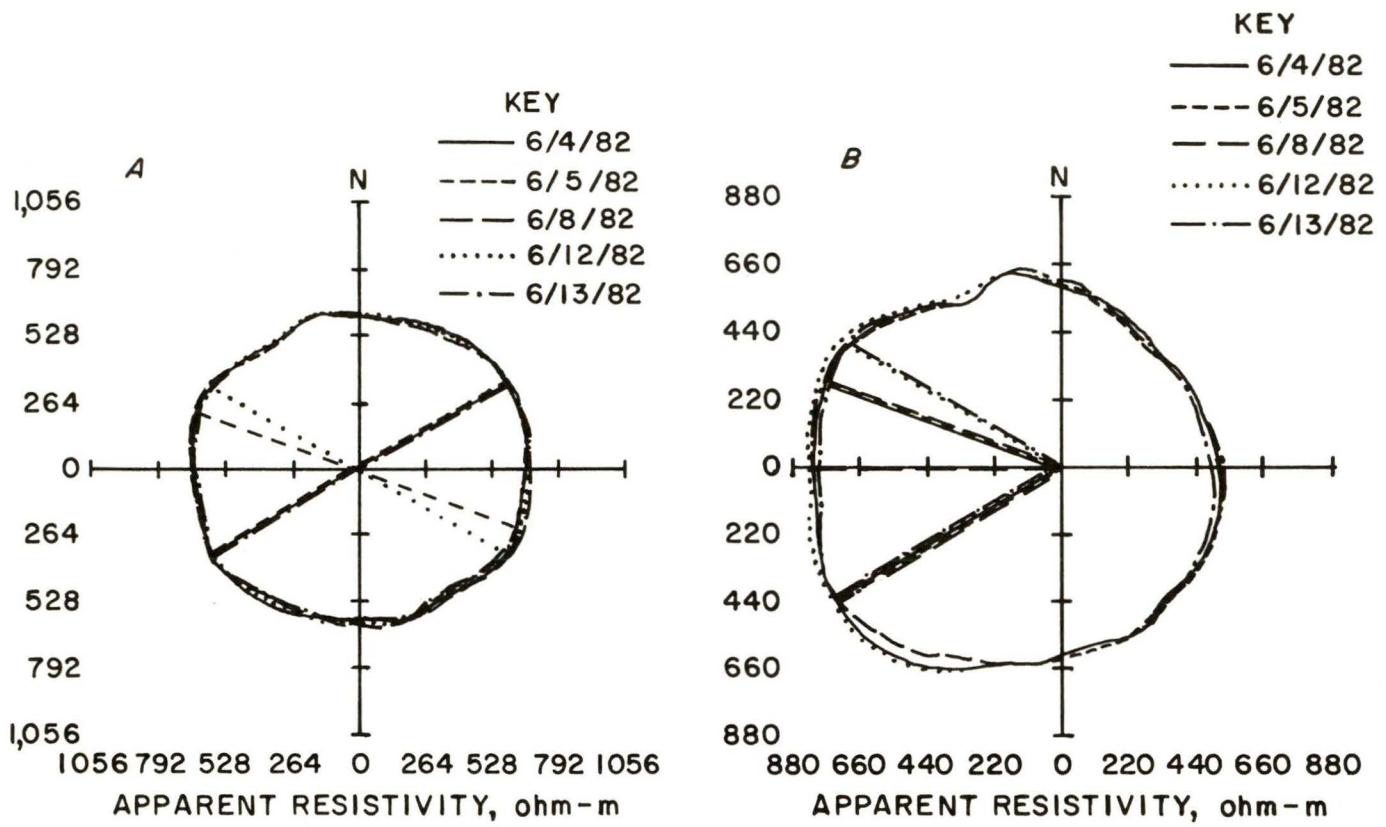


FIGURE 36. - Wenner (*A*) and Lee (*B*) apparent resistivity graphs from azimuthal Wenner-Lee surveys, Beechwood site, Wisconsin, spring 1982 (2).

TABLE 14. - Azimuths of 1982 relative maximum apparent resistivity, Beechwood site, degrees

(13.62-m electrode spacing)

Date.....	6/4	6/5	6/8	6/12	6/13	Date.....	6/4	6/5	6/8	6/12	6/13
Wenner.....	60	60	60	120	60	Lee.....	240	240	240	240	240
	240	110	240	300	240		290	290	270	300	300
	NAp	240	NAp	NAp	NAp		NAp	NAp	290	NAp	NAp
	NAp	290	NAp	NAp	NAp						

NAp Not applicable.

for the area (fig. 31) does not support this explanation, since each of the surveys was done following a dry period of several days. On-site measurement of precipitation and subsurface moisture content are needed to adequately test this hypothesis.

Wenner-Lee surveys were run at Beechwood the following spring. Permanently installed electrodes were used, eliminating any effects of small changes in soil characteristics. The Wenner graphs (figure 36*A* and table 14) have two apparent resistivity maxima, at N60°E and at N110°-120°E. The azimuths do not agree well with the measured joint strike directions. The average apparent resistivities are significantly higher than those measured at the site in the summer, and the graphs are smoother. Lee graphs are asymmetric (fig. 36*B*) with the direction of the asymmetry being in the direction of the dip of the bedrock. The

Wenner-Lee surveys were run over a span of a few days during which there was little time for drying out of joints. There was little precipitation in the area during that time. Therefore, moisture conditions in the vadose zone would not be changing significantly, which would account for the uniform survey results obtained in the spring.

Four azimuthal surveys were run at Neda in 1981. The results show a change in both the direction of the maximum apparent resistivity and in the magnitude of the average resistivity as shown by the size of the graphs (figure 37 and table 15). The azimuth of the apparent resistivity maximum varies from N60°E to N70°E, with additional apparent resistivity peaks at N80°E and at N90°E. The average strike of the northeast trending joints at Neda is N44°E with a standard deviation of 24°. Therefore, the agreement between the azimuthal survey results and the joint survey at Neda is quite poor. One possible explanation for this result is that blasting and mine subsidence fractures were present at the site but not observable at the escarpment. The differential drying of joints according to width could account for the variability of the data as suggested previously.

TABLE 15. - Azimuths of 1981 relative maximum apparent resistivity, Neda site, degrees

(9.14-m electrode spacing)

Date.....	8/21	8/25	9/8	9/13
Wenner.....	60	70	60	60
	90	250	80	240
	240	NAp	240	NAp
	270	NAp	260	NAp

NAp Not applicable.

During the summer, the average apparent resistivity was higher at Neda than at Beechwood by as much as several hundred ohm-meters. Over the same time period, resistivities generally increased at Beechwood but decreased at Neda (compare surveys taken at both sites on the same dates: August 21 and September 13). This result cannot be accounted for at this time. The absence of an apparent resistivity peak corresponding to the known joint set at N141°E cannot be accounted for, nor can the irregularity of the graphs.

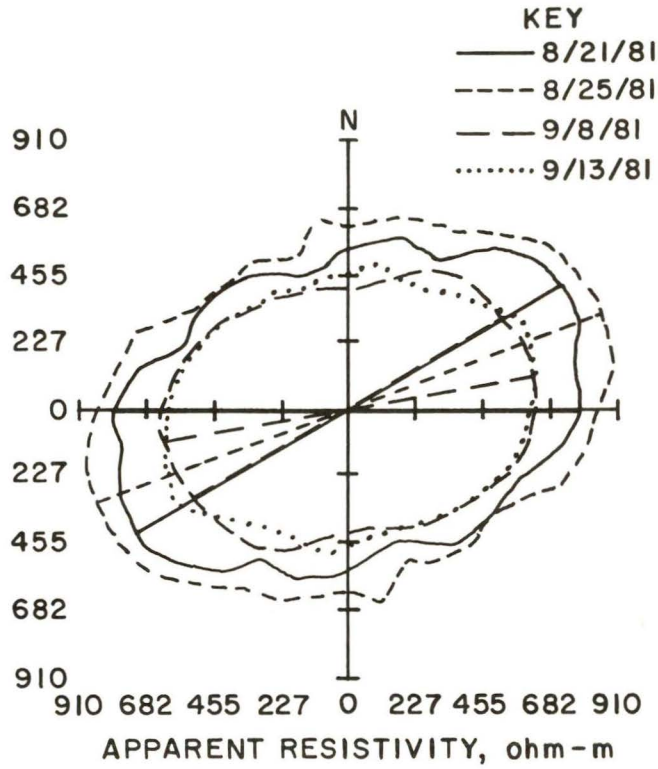


FIGURE 37. - Wenner apparent resistivity graphs from azimuthal Wenner surveys, Neda site, Wisconsin, fall 1981 (2).

Wenner-Lee surveys were run the following spring using permanently installed electrodes. The Wenner graphs (figure 38A and table 16) indicate one apparent resistivity maximum at N70°E, a result similar to that from the summer surveys. The Lee graphs (fig. 38B) are asymmetric, with the direction of the asymmetry to the ENE, while the dip direction is to the east.

Coefficients of anisotropy were calculated from the field data from both sites for graphs which were approximately elliptical. The coefficients of anisotropy (λ) from Neda, the mined site, are consistently higher than at Beechwood. This

agrees with the earlier conclusion that Neda has greater joint and fracture frequency or width, or both, which would increase anisotropy (as long as the fracturing were not totally random). Since the moisture content of the vadose zone is expected to have a significant effect on the resistivity results, values of λ should probably be compared only when data are available for both sites on the same date. SP's were not measured at the Wisconsin field sites.

TABLE 16. - Azimuths of 1982 relative maximum apparent resistivity, Neda site, degrees

(9.14-m electrode spacing)

Date.....	6/9	6/12	6/13
Wenner.....	70	70	70
	250	250	250
Lee.....	260	190	20
	NAp	260	190
	NAp	NAp	260

NAp Not applicable.

Conclusions

Although the Beechwood and Neda sites had a number of advantages over the previous sites (such as a nearby escarpment for joint strike measurements; both mined and unmined areas available for study) the results were not nearly as straightforward. The most reasonable explanation that can be offered at this time is that moisture conditions changed over time in the vadose zone, and the effect was measured in the surface resistivity surveys throughout the study.

At Beechwood and Neda, both the average apparent resistivity and the direction of the maximum apparent resistivity varied over time. This is thought to be the result of a differential drying out of joints of different widths. This can be contrasted with the Spring Valley results where the joints were at or near saturation and the direction of the maximum apparent resistivity was constant over

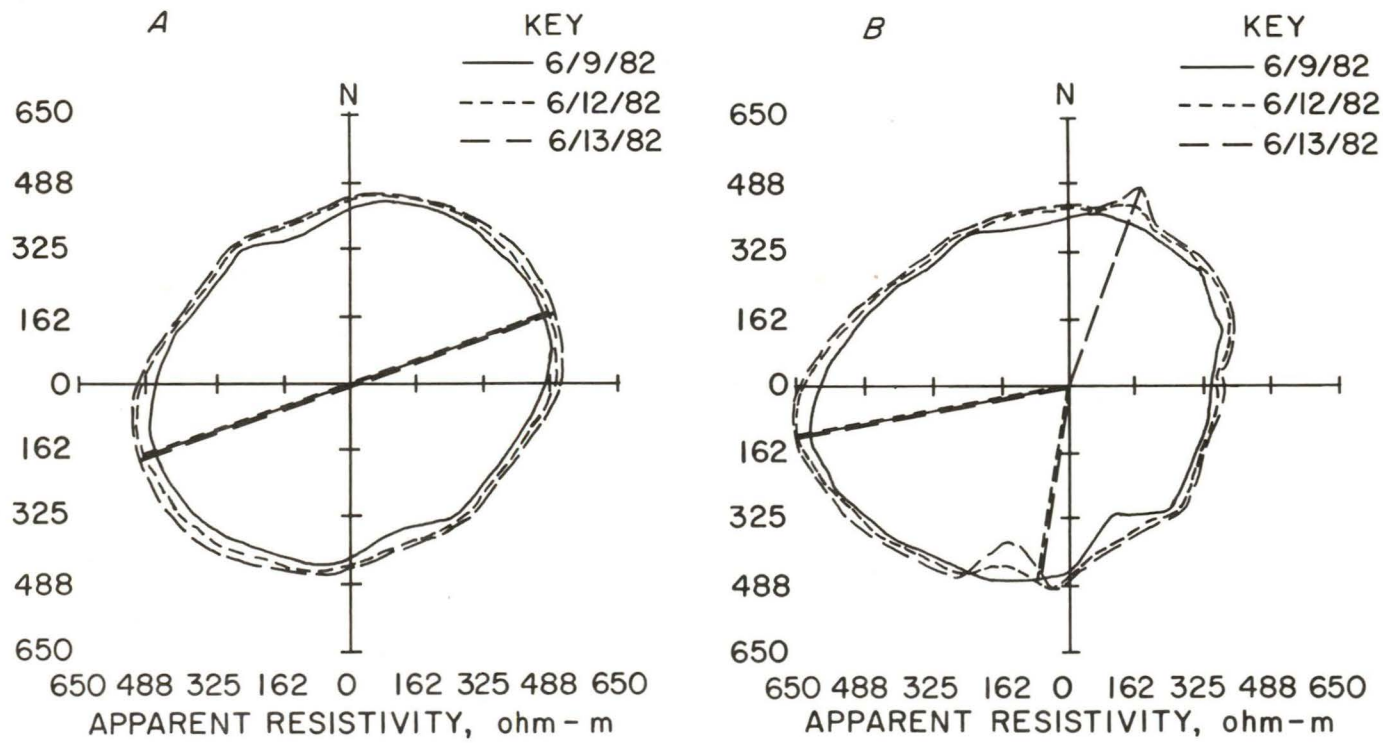


FIGURE 38. - Wenner (*A*) and Lee (*B*) apparent resistivity graphs from azimuthal Wenner-Lee surveys, Neda site, Wisconsin, spring 1982 (2).

time; the change in average apparent resistivity was seasonal and could be attributed to the frost layer.

From the preliminary field tests, the Neda site was found to have greater porosity than Beechwood, and therefore greater joint and fracture frequency or width, or both. Coefficients of anisotropy from the Neda site are greater than at Beechwood and this result can be attributed to the same source (according to equation 24), greater frequency or width of joints and fractures.

MYSTERY RIDGE AND MYSTERY CAVE, FILLMORE COUNTY, MN

Site Descriptions

The Mystery Ridge field site is a farm field approximately 8 miles south and 5 miles east of Spring Valley, MN (SE1/4, sec 20, T 102 N, R 12 W) (refer to figure 9). The ridge extends in a NW-SE direction and has a relatively flat and broad crest. Mystery Ridge is underlain by the Cedar Valley, Maquoketa-Dubuque, and Galena Formations (table 17). The Dubuque is the principal cave-forming limestone in the area and extensive caves, parts of which are open to the public, occur in the Dubuque and the underlying Galena Formation. The orientations of cave passages and intersecting joints have been measured under the ridge in the Dubuque Formation (figs. 39-40). The caves, which are essentially solution enlarged joints, occur principally in the ESE-WNW and NE-SW directions. The orientations of joints intersecting the caves are NE-SW, ESE-WNW, and NW-SE.

The Mystery Cave site is at a picnic area near the entrance to Mystery Cave 1 (SE1/4 sec. 19, T 102 N, R 12 W). The site is approximately three-fourths of a mile southwest of the Mystery Ridge site and is at an elevation about 50 m below the crest of the ridge. There is a thin layer of soil and Dubuque Limestone at the site overlying the Stewartville Member of the Galena Formation. The upper Galena and lower Dubuque Formations are exposed in two quarries near the field site. The joints and bedding are much

TABLE 17. - General geology, Mystery Ridge and Mystery Cave sites, Fillmore County, MN

Depth, m	Formation and/or description
Mystery Ridge:	
0 to 0.30.....	Soil.
0.30 to 3.05.....	Cedar Valley Formation (Devonian); gray to buff or yellow dolomitic limestone.
3.05 to 19.81....	Maquoketa-Dubuque Formation (Ordovician); gray to bluish gray limestone with blue to brown interbedded shale.
19.81 to 35.05...	Maquoketa-Dubuque Formation (Ordovician); gray to bluish gray limestone with blue to brown interbedded shale with greatly enlarged joints and caves.
Below 35.05.....	Stewartville Member, Galena Formation (Ordovician); buff to grayish yellow, fine- to medium-grained dolomitic limestone. Mystery Cave formed in upper Galena, lower Maquoketa Formations.
Mystery Cave:	
0 to 0.30.....	Soil.
0.30 to 1.52.....	Maquoketa-Dubuque Formation (Ordovician); gray to bluish gray limestone interbedded with blue to brown shale.
Below 1.52.....	Stewartville Member, Galena Formation (Ordovician); buff to grayish yellow, fine- to medium-grained dolomitic limestone.

Source: Schwartz, G. M., and G. A. Thiel. Minnesota's Rocks and Water. MN Geol. Surv. Bull. 37, 1963, pp. 137-139.

more closely spaced in the Dubuque than in the Galena (fig. 41). Strike of joint sets in the Stewartville Member at Stewartville, MN have been reported as N58°W, N64°E, N-S, and E-W; the joints are vertical (24).

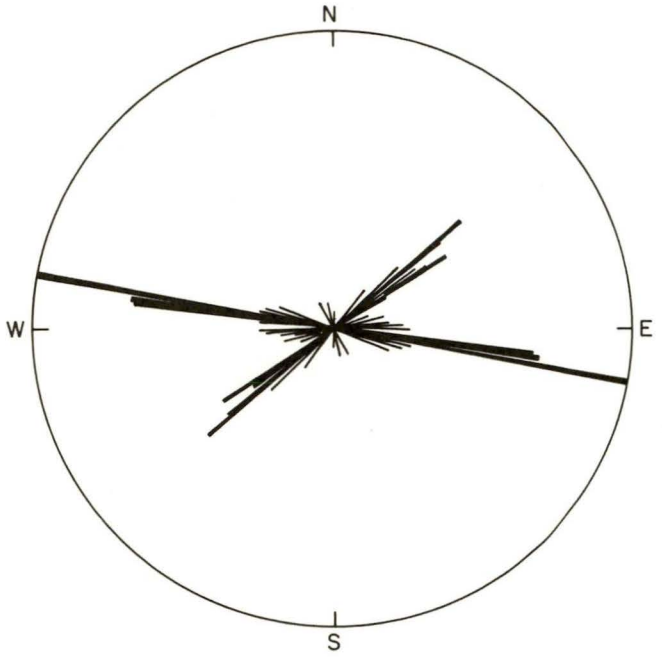


FIGURE 39. - Rose diagram of cave passage orientations, Mystery Ridge, Fillmore County, MN (20).

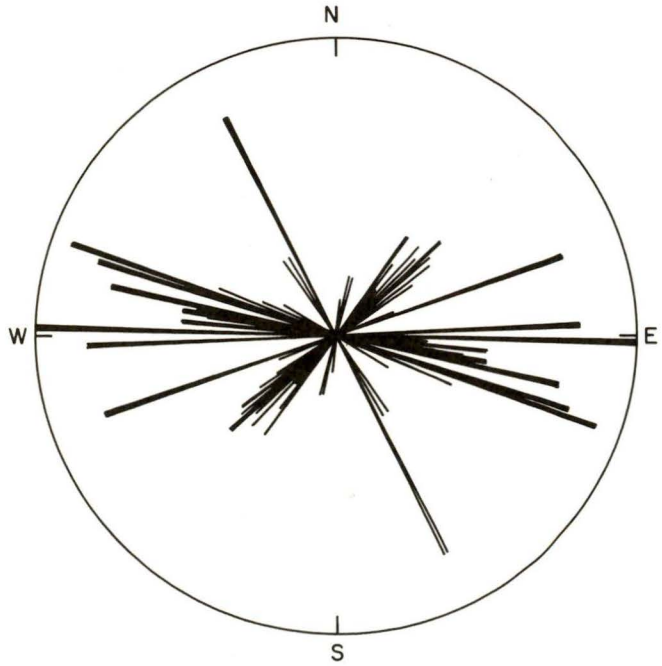


FIGURE 40. - Rose diagram of joint orientations, for joints intersecting cave passages, Mystery Ridge, Fillmore County, MN (20).

The Mystery Ridge site is possibly the most complex of the sites selected for the study. The site includes caves and joints in multiple formations, and may have sinks, perched water tables, unsaturated zones at various depths, and underground rivers. The site was selected because it provided an opportunity to observe the effects of joint width and saturation on apparent resistivity. The caves, which are joints of very large width, occur in one primary direction, ESE-WNW, and one secondary direction, NE-SW, and are air filled.

The fieldwork at the Mystery Ridge and Mystery Cave sites was done in a 2-day period in the spring of 1982. The sites were wet; planting in the fields at Mystery Ridge had not begun because of their saturated condition.

Description of Fieldwork

At the Mystery Ridge site, both the number of azimuthal arrays and the maximum array length were limited by practical considerations. Given the available time, labor, and the size of the ridge crest, electrode spacings of about 15, 30, and 60 m were selected for Wenner-Lee azimuthal surveys. The resistivity system was initially set up at the site but could not be used because of the high natural potentials occurring at the site. An induced polarization (IP) transmitter and receiver were used instead, at a current output of about 1 amp. With that current output, background potential effects were effectively eliminated from the measured apparent resistivity. (The SP could not be measured with the IP equipment, however.) The IP equipment was used for measurements at electrode spacing of 15 and 30 m; on the following day at a site several hundred feet further to the east the background potentials were low and the resistivity system was used there for the 60-m survey. The three surveys have been plotted together,



FIGURE 41. - Quarry near Spring Valley, MN, with Dubuque (upper) and Galena (lower) Formations exposed.

(Courtesy Ms. Pamela Watson)

but it should be kept in mind that the midpoint of the 60-m survey was to the east, and that different equipment was used for the measurements. Measurements were made at 10° intervals at both Mystery Ridge and Mystery Cave.

Results and Conclusions

The most obvious feature of the survey results (figure 42 and table 18) is the great increase in resistivity measured with the 60-m electrode spacing compared with that of the smaller spacings. The direction of the anomaly, NW-SE, corresponds to a joint strike direction in the Maquoketa, Dubuque, and Galena Formations. A maximum apparent resistivity occurs in the NW-SE azimuth on the 15- and 30-m surveys. The predominant cave direction, ESE-WNW, does not correspond to an apparent resistivity maxima on any survey. The joints and/or caves in the NE-SW directions correspond to a maximum apparent resistivity in the 30-m survey.

TABLE 18. - Azimuths of relative maximum apparent resistivity, Mystery Ridge site, degrees

Electrode spacing..m..	15.24	30.48	60.69
Wenner.....	4	54	124
	164	164	184
	184	234	304
	344	344	364
	184	74	124
	224	184	184
	294	234	364
	334	344	NAp

NAp Not applicable.

The caves, which are wide, air-filled joints, have a high resistivity that makes them indistinguishable from the bulk rock matrix, while the smaller joints apparently retain a sufficient amount of water for conduction. This result supports the hypothesis made regarding the differential drying of joints in the vadose zone, presented in the section on the Neda and Beechwood sites.

The shape of the apparent resistivity graphs from the 60-m survey is similar to the shape of the graphs from the Wenner

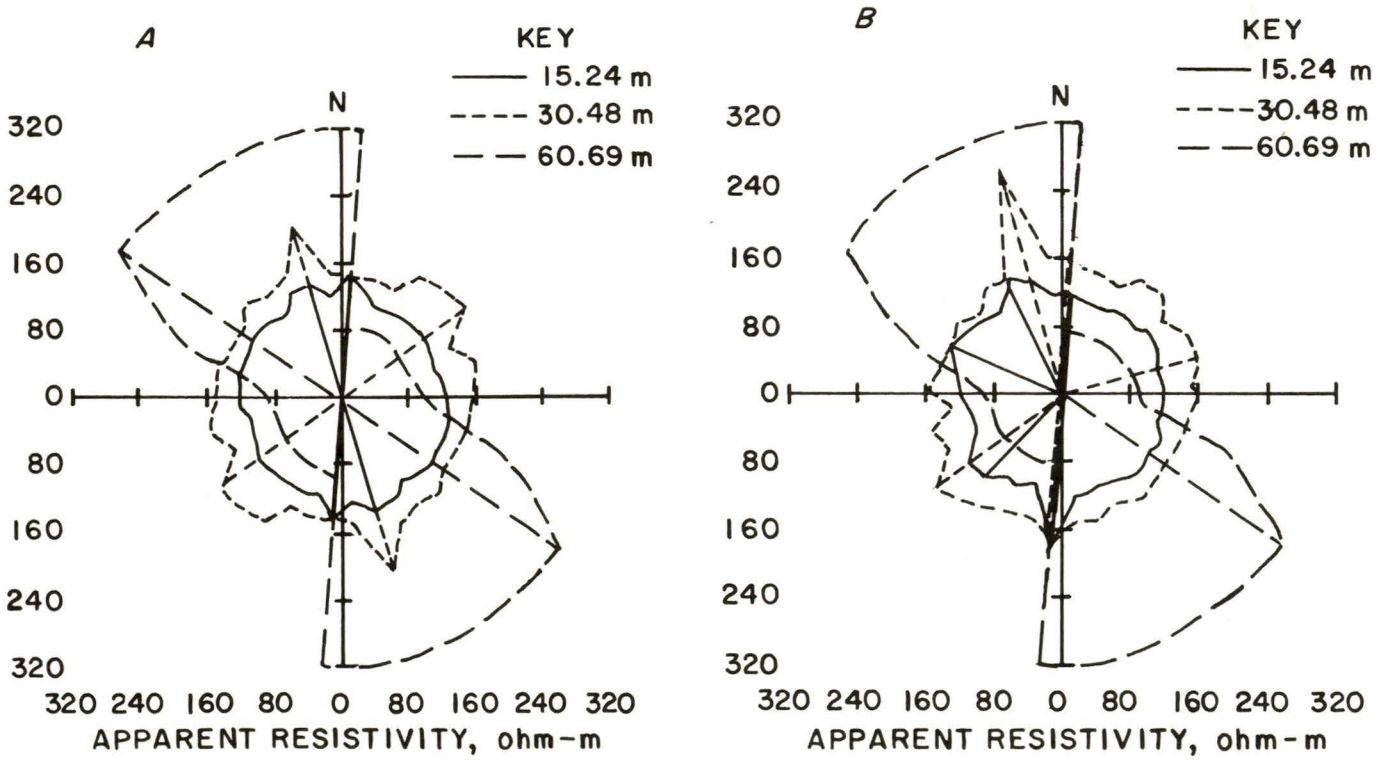


FIGURE 42. - Wenner (*A*) and Lee (*B*) apparent resistivity graphs from azimuthal Wenner-Lee surveys, Mystery Ridge site, Minnesota.

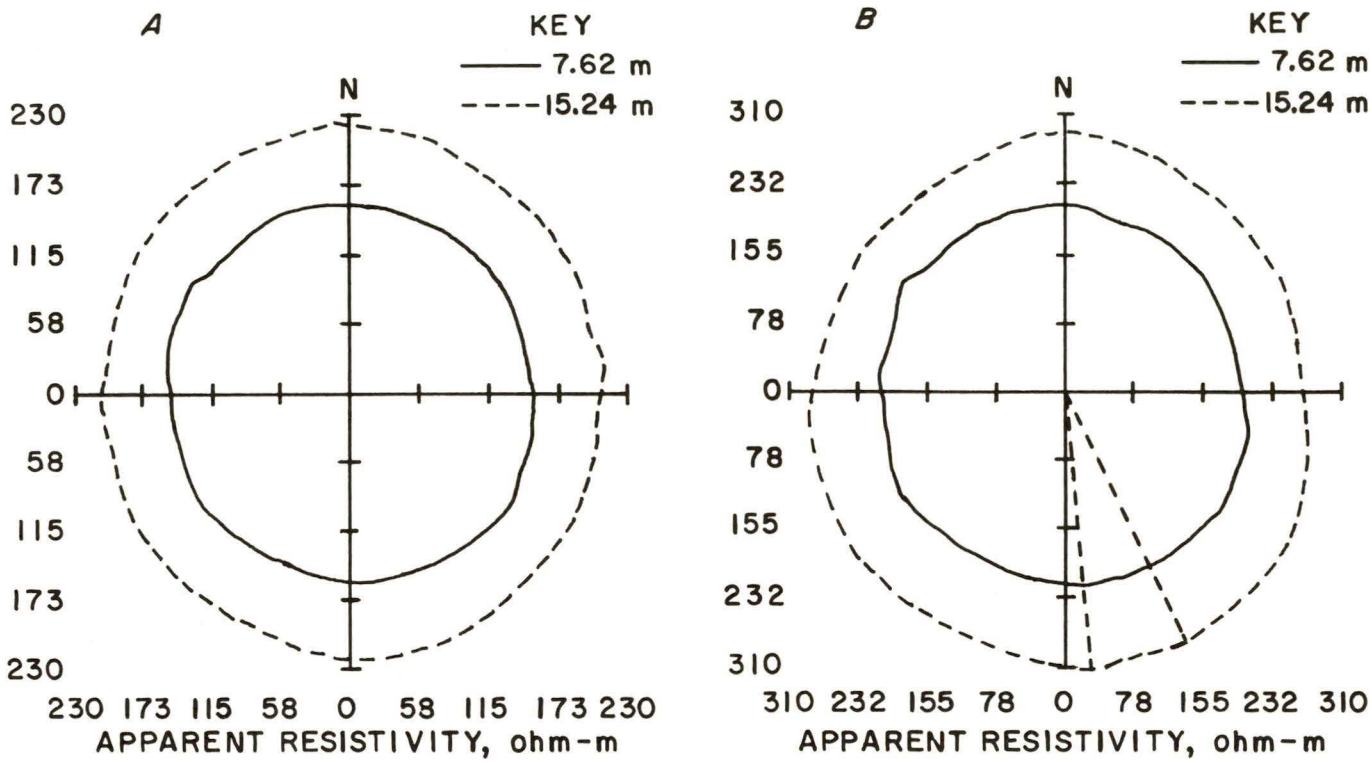


FIGURE 43. - Wenner (*A*) and Lee (*B*) apparent resistivity graphs from azimuthal Wenner-Lee surveys, Mystery Cave site, Minnesota.

surveys completed west of the Spring Valley landfill. The occurrence of high background potentials in the area is another similarity between the sites.

The results of azimuthal surveys at the Mystery Cave site are given in figures 43 and 44 and table 19. According to the landowner, who was present during the survey, the survey was run immediately above a cave in the Stewartville Formation.

TABLE 19. - Azimuths of relative maximum apparent resistivity, Mystery Cave site, degrees

Electrode spacing.....m..	7.62	15.24
Wenner.....	NAp	NAp
Lee.....	NAp	154
	NAp	174

NAp Not applicable.

There are no apparent resistivity peaks in the Mystery Cave graphs. It is not known whether this result is due entirely to dry (air-filled) joints and cave passages, or in part to the wide spacing and small width of the joints in the Stewartville Formation.

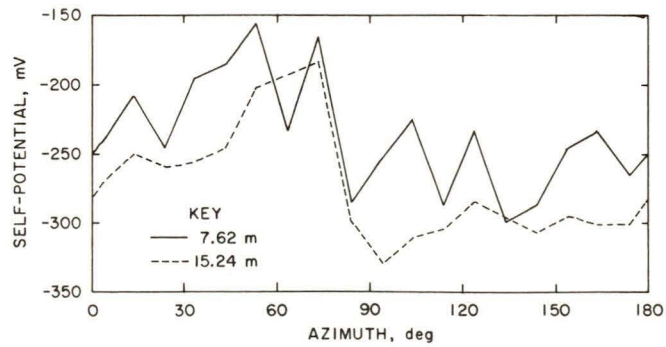


FIGURE 44. - Self-potential, azimuthal survey, Mystery Cave site, Minnesota.

CONCLUSIONS

1. The variation in apparent resistivity with respect to azimuth of near-surface, jointed sedimentary rocks can easily be measured by means of rotated Wenner or Wenner-Lee arrays. The high values of apparent resistivity occur in directions that correspond to known joint strike directions. This relationship is consistent with the theory of resistivity anisotropy (for vertically dipping beds), which states that the maximum apparent resistivity occurs in the direction of strike. In saturated formations, the directions of high apparent resistivities appear to remain constant in time; in unsaturated formations, the directions of high apparent resistivities vary over time. The effect is attributed to the differential drying out of joints in the unsaturated zone during dry periods.

2. The coefficients of anisotropy were calculated from field data for graphs that are approximately elliptical in shape. The coefficients were within the range of values typically found for sedimentary formations. Jointed formations at mined sites have higher coefficients of anisotropy than jointed formations at unmined sites.

3. Zones of ground water inflow through joints or fractures can be delineated by means of horizontal profiling, azimuthal, and self-potential surveys.

4. A general correlation between the asymmetry of the Lee graphs and the dip of bedrock suggests that the method can be used to determine near-surface structure.

This study has shown that the surface resistivity method is an appropriate method for studying joint characteristics. In addition, it has been shown that joints may be treated as very thin layers for analyzing resistivity data. A theory for predicting the apparent resistivity of multiply jointed, multilayered formations and additional field data are needed in order to fully interpret the survey results and to improve upon the methods described.

REFERENCES

1. Ahnell, G., D. R. Buss, R. M. Cohen, and R. R. Parizek. Development of a Dewatering System for Controlling Fracture Dominated Inflow for Acid Mine Drainage Abatement. Final report on BuMines contract H0202002 with Skelly and Loy, May 1983, 210 pp.; available upon request from R. D. Schmidt, Twin Cities Research Center, Bureau of Mines, Minneapolis, MN.

2. Taylor, R. W. Evaluation of Geophysical Surface Methods for Measuring Hydrological Variables in Fractured Rock Units (contract H0318044, Univ. WI--Milwaukee). BuMines OFR 17-84, 1982, 146 pp.; NTIS PB 84-158021.

3. Keller, G. V., and F. C. Frischknecht. Electrical Methods in Geophysical Prospecting. Pergamon, 1966, 519 pp.

4. van Nostrand, R. G., and K. L. Cook. Interpretation of Resistivity Data. U.S. Geol. Surv. Professional Paper 499, 1966, 310 pp.

5. Koefoed, O. Geosounding Principles, 1. Resistivity Sounding Measurements. Elsevier, 1979, 276 pp.

6. Schlumberger, C., M. Schlumberger, and E. G. Leonardon. Some Observations Concerning Electrical Measurements in Anisotropic Media, and Their Interpretation. Tech. Publ. 505, Trans. AIME, v. 110, Geophysical Prospecting, 1934, pp. 3-25.

7. Asten, M. W. The Influence of Electrical Anisotropy on Mise a la masse Surveys. Geophys. Prospect., v. 22, No. 2, 1974, pp. 238-245.

8. Habberjam, G. M. Apparent Resistivity, Anisotropy and Strike Measurements. Geophys. Prospect., v. 23, No. 2, 1975, pp. 211-247.

9. Yakusbovski, U. V., and L. L. Lyaknob. Electrical Prospecting (in Russian). NEDRA, 1964; available from P. G. Chamberlain, BuMines, Minneapolis, MN.

10. Goryunov, I. I., and L. A. Molotkov. Electrical Resistance of Fractured Rock and Its Relationship to Reservoir Properties (in Russian). State Scientific-Technical Publishing House of Petroleum and Mineral-Fuels Literature, Leningrad Dep., Leningrad, Issue 165, 1961, pp. 237-247; English translation available upon request from Librarian, BuMines, Minneapolis, MN.

11. Goryunov, I. I. Electrical Resistivity of Fractured Rock (in Russian). Appl. Geophys., Issue 38, 1964, pp. 173-179. English translation available upon request from P. G. Chamberlain, BuMines, Minneapolis, MN.

12. Dutta, N. P., R. N. Bose, and B. C. Saikia. Detection of Solution Channels in Limestone by Electrical Resistivity Method. Geophys. Prospect., v. 18, No. 3, 1970, pp. 405-414.

13. Rainert, E. R. The Effects of Anisotropic Media on Resistivity Prospecting. Thesis, School of Earth Sciences, Macquarie University, North Ryde, New South Wales, 1972, 169 pp.

14. Wilson, C. R., and P. A. Witherspoon. Steady State Flow in Rigid Networks of Fractures. Water Resour. Res., v. 10, No. 2, April 1974, pp. 328-335.

15. Parkhomenko, E. I. Electrification Phenomena in Rocks (in Russian). English translation, Plenum, 1971, 285 pp.

16. Ogilvy, A. A., M. A. Ayed, and V. A. Bogoslovsky. Geophysical Studies of Water Leakages From Reservoirs. Geophys. Prospect., v. 17, No. 1, 1969, pp. 36-62.

17. Ogilvy, A. A. Geophysical Prospecting for Groundwater in the Soviet Union. Paper in Mining and Groundwater Geophysics, ed by L. W. Morley (Proc. of the Canadian Centennial Conf. on Mining and Groundwater Geophysics, Niagara Falls, Canada, Oct. 1967). Geol. Survey of Canada, Economic Geol. Rep. No. 26, 1967, pp. 536-543.

18. Bogoslovsky, V. A., and A. A. Ogilvy. The Study of Streaming Potentials on Fissured Media Models. Geophys. Prospect., v. 20, No. 1, 1972, pp. 109-117.

19. Minnesota Highway Department., Office of Materials. Laboratory Log and Test Results, Bridge No. 4477, 1977, 6 pp.

20. Alexander, C. Unpublished data, 1982; available upon request from C. Alexander, Dep. Geol. and Geophys., Minneapolis, MN.

21. Mohr, R. E., and J. E. Pizzato. The Analysis of Joint Orientation Systematics in a Small Area of SE Minnesota. Unpublished manuscript, Nov. 1978; available upon request from C. Alexander, Dep. Geol. and Geophys. Univ. MN, Minneapolis, MN.

22. Kohls, D. W. Lithostratigraphy of the Cedar Valley Formation in Minnesota and Northern Iowa. Ph. D. Thesis, Univ. MN, Minneapolis, MN., June 1961, pp. 27-28.

23. McCulloch, C. M., W. P. Diamond, B. M. Bench, and M. Deul. Selected Geologic Factors Affecting Mining of the Pittsburgh Coalbed. BuMines RI 8093, 1975, 72 pp.

24. Larson, W. C., and J. M. Pugliese. Effects of Jointing and Bedding Separation on Limestone Breakage at a Reduced Scale. BuMines RI 7863, 1974, 13 pp.

APPENDIX.--NOMENCLATURE

ρ_{a_ℓ}	apparent longitudinal resistivity, ohm-meters
ρ_a	apparent resistivity, ohm-meters
ρ_{a_t}	apparent transverse resistivity, ohm-meters
A	area, square meters
λ	coefficient of anisotropy, dimensionless
I	current, amperes
x, y, z, L, r	distance, meters
a	electrode spacing, meters
σ_ℓ	longitudinal conductivity, 1/ohm-meters
ρ_ℓ	longitudinal resistivity, ohm-meters
K	permeability, centimeters per second
ϕ	porosity, percent
V	potential difference, volts
U	potential, volts
ρ	resistivity, ohm-meters
H, h	thickness, meters
S	total conductance, 1/ohm
T	transverse resistance, ohms
ρ_t	transverse resistivity, ohm-meters
R	resistance, ohms

☆U.S. GPO: 1984-705-020/5047

INT.-BU.OF MINES,PGH.,PA. 27687